

Zinc-Directed Inhibitors for Zinc Proteinases

BY H. FEINBERG, H. M. GREENBLATT, V. BEHAR, C. GILON, S. COHEN, A. BINO AND G. SHOHAM*

Institute of Chemistry and The Laboratory of Structural Chemistry and Biology, The Hebrew University of Jerusalem, Jerusalem 91904, Israel

(Received 19 August 1994; accepted 7 March 1995)

Abstract

Zinc proteinases have been recognized as a distinct class of proteolytic enzymes in which at least one ion of zinc is involved directly in catalysis. This family includes a growing number of biologically important enzymes which are attractive targets for rational drug design. In this paper we examine the special features of the zinc binding environment of these enzymes in order to gain information which could be useful in the preparation of 'zinc-directed' selective inhibitors. Carboxypeptidase A (CPA) is presented as a model for one class of zinc proteinases, and the active-site zinc and its interactions are examined with the primary focus on geometrical considerations. The three-dimensional structure of the native and apoenzyme are discussed, together with the high-resolution structure of several enzyme–inhibitor complexes. This paper will first present a structural analysis of CPA derivatives and then discuss a series of zinc model compounds which have been prepared and characterized in order to examine the ligand and geometrical preferences of the zinc in an unstrained system. X-ray crystallography (macromolecular and small molecule) is the main experimental method used for the structural analyses, while complementary computational methods have been used for the examination of electrostatic potentials. The results from the various experimental efforts are assembled in order to draw general conclusions on the potential use of the zinc ion as the primary target for inhibitor binding. The results of these studies suggest that the zinc ion is important for both the binding and the catalytic activation of the substrate as well as for stabilization of the tetrahedral reaction intermediate.

Introduction

Zinc is one of the most biologically significant transition metals and has been shown to play an important role in correct enzymatic function (Vallee, Galdes, Auld & Riordan, 1983; Vallee & Galdes, 1984). Although zinc can play either a catalytic, structural or regulatory role, it generally participates directly in catalysis (Vallee *et al.*, 1983). Zinc-containing polypeptides, which are found

in all six classes of enzymes, take part in biological reactions encompassing a wide range of metabolic events. A subgroup of zinc enzymes, known as zinc proteinases (also termed 'zinc proteases' and 'metalloproteinases'), has recently been the subject of extensive biochemical and biophysical study. Zinc proteinases contain at least one zinc ion which has a direct role in proteolysis (Vallee, 1986; Vallee & Galdes, 1984). For many years high-resolution crystal structures were available for only two such enzymes, thermolysin (TLN, 1.6 Å) (Holmes & Matthews, 1982) and carboxypeptidase A (CPA, 1.5 Å) (Rees, Lewis & Lipscomb, 1983). Carboxypeptidase B (CPB) (Schmid & Herriot, 1976), was studied at 2.8 Å resolution, and its C α structure is available. A D-alanyl-D-alanine cleaving carboxypeptidase [also called peptidase G, PEP-G (Dideberg *et al.*, 1982)][†] has been studied at 2.5 Å resolution.

Of late there has been a significant increase in the number of reported three-dimensional crystal structures of zinc proteinases from a variety of biological sources, with various biological functions and target specificities. Such structures include, among others, the X-ray crystal structures of the following: *Bacillus cereus* neutral protease (NPC) at 2.0 Å resolution (Pauptit *et al.*, 1988; Stark, Pauptit, Wilson & Jansonius, 1992), *Psuedomonas aeruginosa* elastase at 1.5 Å resolution (Thayer, Flaherty & MacKay, 1991), the digestive enzyme astacin from crayfish at 1.8 Å resolution (Bode, Gomis-Rueth, Huber, Zwilling & Stocker, 1992; Gomis-Rueth, Kress & Bode, 1993), the snake venom metalloproteinase adamalysin II at 2.0 Å resolution (Gomis-Rueth, Stocker, Huber, Zwilling & Bode, 1993), the catalytic domain of human fibroblast collagenase at 2.2 Å resolution (Borkakoti *et al.*, 1994; Lovejoy *et al.*, 1994), mature truncated human fibroblast collagenase at 1.5 Å resolution (Spurlino *et al.*, 1995), the catalytic domain of human neutrophil collagenase at 2.0 Å resolution (Bode *et al.*, 1994; Stams *et al.*, 1994), carboxypeptidase A2 from rat at 1.94 Å resolution (Faming, Kobe, Rutter & Goldsmith, 1991), carboxypeptidase T from *Thermoactinomyces vulgaris* at 2.35 Å (Teplyakov *et al.*, 1992), neutral protease from *Streptomyces caespitosus* (main chain) (Harada, Kita-

[†] The structure of D-alanyl-D-alanine-cleaving carboxypeptidase (PEP-G) has been recently refined at 1.8 Å resolution, J. P. Wery, personal communication.

* Author for correspondence.

dokoro, Kinoshita, Kai & Kassai, 1991), alkaline metalloproteinase from *Pseudomonas aeruginosa* at 1.64 Å resolution (Baumann, Wu, Flaherty & McKay, 1993), and the NMR structure of the inhibited catalytic domain of human stromelysin 1 (Gooley *et al.*, 1993, 1994). The detailed crystal structures of the related co-catalytic zinc aminopeptidases, leucine aminopeptidase (Burley, David, Sweet, Taylor & Lipscomb, 1992; Kim & Lipscomb, 1993) and *Aeromonas proteolytica* aminopeptidase (Chevrier *et al.*, 1994), have also been determined recently at 2.7 and 1.8 Å resolution, respectively.

Analysis of the structures of mono-zinc proteinases indicates that the family could be structurally divided into two general folds: the CPA-type fold (representative of exoproteinases) and the thermolysin-type fold (representative of endoproteinases). The group comprising the thermolysin-type fold can itself be subdivided according to the type of zinc-binding motif: the thermolysin subgroup (HExxH motif) and the astacin subgroup (HExxHxxGxxH motif) (Blundell, 1994). Despite the differences in folds, zinc-binding motifs and active-site topologies, all of these enzymes have a catalytic zinc(II) ion at the active site where three of the coordination sites are occupied by protein ligands and the fourth coordination site is labile, and serves for the binding of substrate and catalysis (Vallee & Auld, 1993*a,b*). Recent structural data suggest that despite the existence of different metal-binding motifs, the zinc proteinases show similar modes of substrate-zinc binding and metal utilization during catalysis. It is these features of zinc proteinases that could ideally be exploited for rational drug design. A present research goal is to use the catalytic zinc present in these enzymes as the initial binding target of inhibitors in order to achieve preferred binding to zinc proteinases over other enzymes, especially serine proteinases which are more common in number and concentration than are other proteinases. Such binding to zinc is hoped to provide a strong anchor to the incoming inhibitor/drug which will then be fixed in position and orientation by other residues in the active site. Once the inhibitor is directed to zinc proteinases its specificity and selectivity to a particular enzyme in the family can be modulated by the introduction of additional functional groups which will interact with the substrate-binding subsites. That is, an ideal inhibitor for a specific zinc proteinase should be constructed of two different components: a zinc-directed component and a substrate-specificity component. The substrate-specificity components would be designed not only to improve the relative selectivity for a given target but also to increase the absolute affinity of the inhibitor for a particular enzyme. These additional specific interactions could contribute greatly to the overall binding of the inhibitor and, in ideal cases, decrease the inhibition constant to the nanomolar range or less. The main point of consideration in the present paper, however, is the zinc-directed component of metalloproteinase inhibitors.

Carboxypeptidase A

In order to examine closely the detailed geometry of the catalytic zinc-binding pocket in both uncomplexed (native) and complexed zinc proteinases we selected a particular subset of enzymes according to the specific ligands of their catalytic zinc ion. This subset includes those enzymes which in their native form have zinc liganded by two histidine side chains, a glutamate carboxylate and a water molecule. This subset of the zinc proteinase family is referred to below as the ZP-H2E subgroup in contrast to the other subset of enzymes containing three histidines as ligands to the catalytic zinc (referred to below as the ZP-H3 subgroup). There are four enzymes

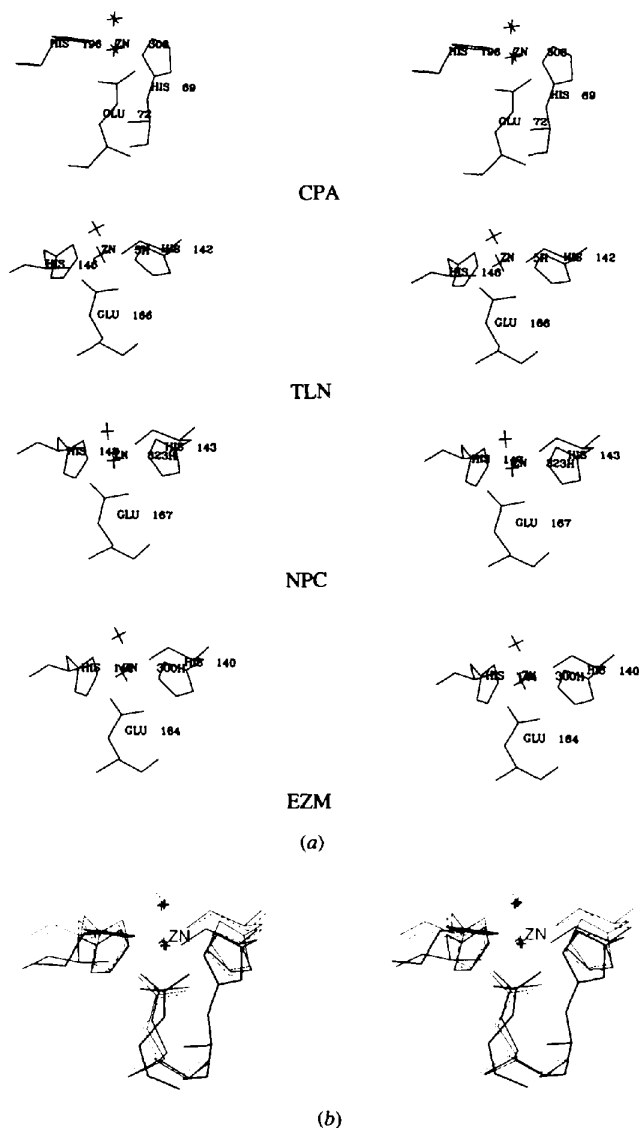


Fig. 1. (a) The active site of four zinc proteinases of the ZP-H2E subgroup (where zinc is liganded to two histidines and one glutamate) for which the crystal structure is available. (b) Superposition of the active sites of the four ZP-H2E enzymes: triple line, CPA; double line, TLN; single line, NPC; dashed line, EZM.

from the ZP-H2E subgroup for which three-dimensional coordinates are currently available: carboxypeptidase A (CPA) (Rees *et al.*, 1983), thermolysin (TLN) (Holmes & Matthews, 1982), *B. cereus* neutral protease (NPC) (Stark *et al.*, 1992), and *P. aeruginosa* elastase (EZM) (Thayer *et al.*, 1991). The zinc coordination spheres of these four enzymes are shown in Fig. 1(a). A least-squares fit of the zinc ion and its ligands demonstrates that the geometry about the zinc ions is virtually identical in the four structures. This conclusion is significant as the overall structures themselves display important differences which could have differential effects on the torsional strain placed on the zinc ion and its proteinaceous ligands (Vallee *et al.*, 1983).

As these structures are generally similar with regard to zinc coordination, we decided to take one enzyme as a model for the ZP-H2E subgroup. Of these enzymes, CPA was the enzyme of choice since its structure is the most accurately determined (as reflected in crystallographic resolution and *R* factor), it is the most thoroughly studied (both in terms of structure and function) and it is the most convenient to use experimentally (commercially available, stable crystals and readily available inhibitors). The zinc-liganding amino-acid side chains are nearly identical (Fig. 1b) among TLN, NPC and EZM which also share considerable sequence homology. In comparison with these enzymes, the zinc ligands in CPA seem to differ in their spatial distribution, which is expected considering the low sequence homology to the other enzymes; however, the relative positions of the zinc-binding atoms are very similar and the zinc coordination spheres from the two sets of enzymes can be closely superimposed (Fig. 1b).

The biochemical and structural aspects of CPA are summarized in a number of reports and recent reviews (Lipscomb, 1980; Vallee *et al.*, 1983; Vallee & Galdes, 1984; Christianson & Lipscomb, 1989; Feinberg, Greenblatt & Shoham, 1993). The enzyme contains one zinc ion per molecule which is absolutely required for activity. CPA is a monomer of molecular weight of 34 500 Da (307 amino acids). Complexes with inhibitors and analogues (Rees & Lipscomb, 1982, 1983; Christianson & Lipscomb, 1985a,b, 1986a,b, 1987; Christianson, David & Lipscomb, 1987; Shoham, Christianson & Oren, 1988; Christianson, Mangani, Shoham & Lipscomb, 1989; Kim & Lipscomb, 1991; Mangani, Carloni & Orioli, 1992a,b; Mangani & Orioli, 1992) and enzyme structures at various pH conditions (Shoham, Rees & Lipscomb, 1984) are available from high-resolution crystallographic studies. CPA catalyzes the hydrolysis of the carboxy-terminus residue of peptides and carboxyesters, and exhibits specificity towards substrates bearing a large hydrophobic C-terminal residue such as phenylalanine. The zinc ion, situated in the active site, is penta-coordinated by the N^{δ1} atoms of two histidine residues (His69, His196), the two O^ε atoms of a glutamic acid residue (Glu72), and one molecule of water. Bovine CPA readily forms

large and stable crystals which diffract to high resolution. These crystals show one-third the peptidase activity of CPA in solution (Quiocho & Richards, 1966; Quiocho, McMurray & Lipscomb, 1972), indicating that the enzyme in the crystal has a similar structure to the solution species. Such similarity is of great importance if one is to use crystallographic results to design molecules which will react with the enzyme in solution; other data also suggest that the enzyme in the crystal and in solution adopts similar conformations (Lipscomb, 1980; Shoham *et al.*, 1984).

Intensive biochemical and biophysical characterization of CPA has been performed by numerous research groups (Vallee & Galdes, 1984; Christianson & Lipscomb, 1989) and most of the functional groups essential for catalysis have been identified. Still, the precise mechanism of action of the enzyme remains ambiguous (Feinberg *et al.*, 1993). At the present time it appears that at least three functional groups of the enzyme are directly involved in substrate hydrolysis: the carboxylic group of glutamate 270 (Glu270), the zinc ion, and a zinc-coordinated water molecule (Lipscomb *et al.*, 1968). While the role of the guanidinium group of Arg127 is not clear, recent data suggest that this group may play an important role in binding and catalysis (Christianson & Lipscomb, 1986a,b, 1987, 1989; Christianson *et al.*, 1987; Shoham, Christianson *et al.*, 1988; Phillips, Fletterick & Rutter, 1990; Feinberg *et al.*, 1993). Other amino-acid residues participate indirectly in catalysis and some may be involved in binding of substrate in the proper orientation in the active site. These residues include Arg71, Tyr198, Asn144, Arg145, Tyr248 and Phe279. Ser197 and Asp142 establish hydrogen bonds to active-site functional groups (Rees *et al.*, 1983) and may be involved in either binding or catalysis. Kinetic experiments have shown that the substrate-binding region extends to five amino acids, and that hydrolysis of longer substrates does not deviate significantly from Michaelis-Menten kinetics (Abramowitz, Schechter & Berger, 1967).

As described previously, the present paper will focus on the zinc environment of CPA and its direct involvement in the binding of substrates and inhibitors. Although zinc coordination plays an important role in the catalytic reaction of the enzyme, we will not address herein the questions related to the mechanism of CPA and zinc proteinases which are discussed elsewhere (Christianson & Lipscomb, 1989; Feinberg *et al.*, 1993). It should be noted that in spite of the ambiguous data regarding the catalytic reaction of CPA, the general features of zinc binding outlined here are useful for inhibitor/drug design for zinc proteinases of yet unknown structure. The list of such enzymes includes important enzymes such as angiotensin converting enzyme (blood pressure regulation) (Soffer, 1976) and enkephalinase (neuropeptide processing) (Malfroy, Swerts, Guyon, Roques & Schwartz, 1978; Schwartz,

Table 1. *Data measurement and refinement parameters for native CPA and apo-CPA*

	Native CPA	Native CPA*	Apo-CPA
Detector	Nicolet P2 ₁	R-AXIS-IIC	DIP-100
No. of crystals	3	1	1
Independent reflections	32080	34352	21540
$R_{\text{merge}}/R_{\text{sym}}$ (%)	10	4	8
No. of refinement cycles	51	36	32
No. of water molecules	192	213	184
R.m.s. deviation (σ -target)			
Bond lengths	0.024 (0.017)	0.017 (0.015)	0.013 (0.015)
Average w ($^{\circ}$)	8.5 (6.4)	2.8 (2.5)	2.3 (2.5)
Final r.m.s. coordinate shifts		0.013	0.016
Resolution (\AA) (cutoff on F)	1.54	5.00–1.53 (2σ)	8.00–1.90 (0σ)
Final R factor (%)	19.0	14.8	15.8

* The newly refined native CPA structure.

Gros, Lecomte & Bralet, 1990), as well as a number of other enzymes which are involved in medically significant metabolic processes.

High-resolution structures of native and apo-CPA

The original refined high-resolution structure of CPA (Rees *et al.*, 1983) was the product of single counter diffractometer data sets which were measured on several crystals and gathered over the course of several years of study. In addition, it was found recently from a bovine cDNA sequence of CPA (Shoham, Nechushtai, Steppun, Nelson & Nelson, unpublished results; Le Hurou, Guilloteau, Toullec, Puigserver & Wicker, 1991) that there are seven incorrect assignments of amino-acid side chains (Asp/Asn and Glu/Gln) in the originally determined polypeptide sequence (Neurath, Bradshaw, Pétra & Walsh, 1970). Some of these errors were previously noted by Pétra, Hermodson, Walsh & Neurath (1971). These errors are not uncommon when amino-acid sequences are determined by protein sequencing and in the case of CPA the mistakes did not include critical catalytic amino-acid residues. Nevertheless, in the process of refinement of a structure at atomic resolution such small sequence corrections may be of significance in the interpretation of hydrogen-bond configurations.

Our initial goal in the structure/activity study of CPA was to obtain the best possible high-resolution structure of the native enzyme; our method involved the collection of higher quality area-detector diffraction data from a single crystal and a model refined with the corrected

sequence. This work was undertaken in order to provide the best possible reference structure for inhibitor-binding studies, since the changes in the atomic positions for these enzyme complexes may be small.

Diffraction data from one native CPA crystal were collected to 1.48 \AA resolution on a Rigaku R-AXIS IIC imaging-plate area detector (Shibata, 1990; Sato *et al.*, 1992), using graphite-monochromated Cu $K\alpha$ radiation. The enzyme structure was then refined using restrained least-squares methods (Hendrickson & Konner, 1981). The data collection details and the results of the refinement are summarized in Table 1. The improvement in the quality of the model is apparent from a comparison of the R factors and geometry parameters between the older and more recent CPA models (discussed in detail in Greenblatt *et al.*, 1995). Inclusion of water molecules in the final structure was also subject to stringent criteria, as residual peaks in the electron-density map were not assigned as water molecules unless the height of the peak was at least three times that of the root-mean-square (r.m.s.) deviation of the map, and occupied more than one grid point in space.

In order to clarify what role the metal might play in the maintenance of the structure of CPA, and in catalysis, the metal ion was extracted from crystals of CPA, yielding apo-CPA (Greenblatt *et al.*, 1995). Atomic absorption data showed that virtually all the zinc (>99%) had been extracted from the crystals. The crystals of apo-CPA were subjected to a full structural analysis. Diffraction data were collected to high resolution (1.9 \AA) and the resultant model was refined to a final R factor of 15.8%. As is apparent from Table 1, the quality of this structure is comparable to the quality of the model of the native enzyme, and thus meaningful conclusions may be drawn from even small (~ 0.2 \AA) changes in the structure.

In general, the structure of apo-CPA is very similar to that of the native enzyme as reported in earlier lower resolution studies (Rees & Lipscomb, 1983). As demonstrated in Fig. 2, the only major structural effect of zinc removal was that one zinc ligand, His196 rotated 110 $^{\circ}$ about χ_2 , to form a salt bridge with Glu270. These results suggest that the zinc ion does not play a very large role in maintaining the overall native conformation of CPA and that the zinc ion maintains only a small part of the enzyme conformation at the active site. One may

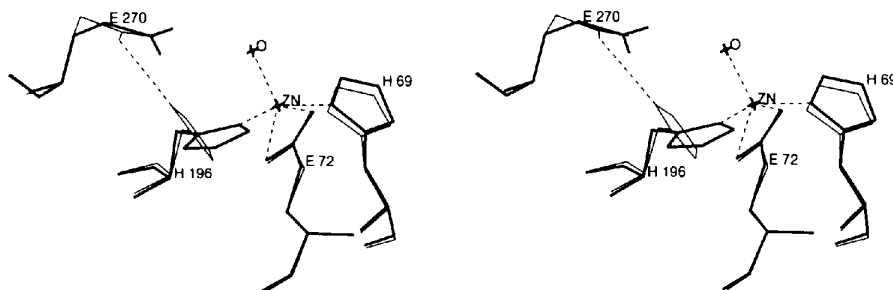


Fig. 2. A comparison of the active site of native CPA (thick lines) and apo-CPA (thin lines), showing little overall change in the conformation of the side chains in the vicinity of the zinc. The major exceptions are His196 and Glu270 which now form a salt bridge (distance shown is 2.9 \AA).

then conclude that the loss of activity observed upon removal of the zinc ion is due to the absence of the metal alone, and not because of large structural changes.

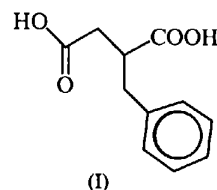
In order to examine what role the zinc ion might play in binding substrates, attempts were made to complex apo-CPA with inhibitors and analogues. It was hoped that information about the possible roles of other active-site functional groups in binding substrate might be revealed. Moreover, the structure of the apoenzyme with an inhibitor, or a substrate, might yield a model for the Michaelis–Menten (pre-catalytic) complex. Analysis of the structure of the Michaelis–Menten complex is especially relevant in determining whether or not different types of substrates have different initial binding modes. High-resolution data sets were collected on a series of crystals of the apoenzyme which had been soaked with several high-affinity substrates and inhibitors (ketomethylene and benzyl-succinate derivatives, as described below). These structures were then refined to convergence (with final R factors of less than 17%). It was an interesting result to find that in this series of refined structures (of potential apo-CPA complexes) none of the inhibitors, nor any of the peptide substrates was seen bound in the active site, even when the soaking was performed in millimolar concentrations, close to the solubility limit of these compounds.

A possible reason for the lack of binding is that the soaking concentration was, nevertheless, too low. One would expect that the upper limit for the association constant of peptide substrates with apo-CPA should be no better than the K_m of these compounds in the native enzyme. This is consistent with the results of Coleman & Vallee (1962) who showed that the inhibition constant for some common peptide substrates which prevented binding of zinc to apo-CPA to be close to, but larger than their K_m values. This decrease in affinity suggests that zinc does contribute, perhaps indirectly, to the formation of the Michaelis–Menten complex of CPA even with peptide substrates. Although the dipeptide Gly-Tyr has been shown to bind to apo-CPA (Rees & Lipscomb, 1983) this molecule binds in an anomalous fashion to native CPA, and so may not be representative of other substrates.

Complexes of metallo-CPA derivatives with benzyl succinate inhibitor

A relatively small inhibitor with simple inhibitory characteristics, benzyl succinate [(I)], was chosen for analysis of the interactions of the enzyme with an inhibitor. (I) shows high affinity to CPA (Byers & Wolfenden, 1972, 1973) and has been the starting point for much effort in drug design for zinc proteinases (Cushman, Ceung, Sabo & Ondetti, 1977; Patchett *et al.*, 1980; Martin, Holmquist & Riordan, 1989). In fact, (I) represents a family of dicarboxylate anions, all of which are competitive inhibitors of CPA (Byers & Wolfenden, 1972;

Bicknell *et al.*, 1988). Among these compounds (I) is the most potent inhibitor for both peptide and ester hydrolysis ($K_i = 4.5 \times 10^{-7} M$) (Byers & Wolfenden, 1973). The high affinity of (I) to CPA has been explained by its resemblance to the products of peptide hydrolysis and was, therefore, considered originally as a 'biproduct analogue' (current data shows that it seems to resemble better an intermediate or TS analogue, as discussed below). It contains a moiety analogous to the terminal amino acid (L-phenylalanine) which is cleaved, and an additional carboxylate group that was thought to resemble the carboxy terminus of the newly shortened peptide. We present here a summary of the structural results obtained from the complexes of benzyl-succinate with native (zinc) CPA, Hg-CPA and Ni-CPA. These metal derivatives of CPA were studied in order to examine whether metal substitution has an effect on substrate/inhibitor binding with specific emphasis on the general nature of interactions of an active-site divalent metal ion with carboxylic inhibitors.



Crystals of CPA metal derivatives were prepared by soaking crystals of the apoenzyme with the corresponding chloride salts of a given metal (Maret, 1986; Bertini, Luchinat & Viezzoli, 1986; Feinberg *et al.*, 1993). Special care was taken to purge all the solutions involved in the metal-exchange procedure of any (trace) metal impurities. In all cases it was confirmed by atomic absorption that at least 98% of the active-site zinc was replaced with the metal ion of interest. The complex of native CPA and (I) as well as the complexes of Ni-CPA/(I) and Hg-CPA/(I) were prepared by soaking the appropriate CPA crystals in benzyl succinate solutions. In all three electron-density maps, (I) was found in the active site at close to full occupancy while the crystals used for data collection were found to be isomorphous with the original CPA crystals and diffracted to high resolution. Experimental conditions for preparing all three complexes were kept similar in order to minimize solution effects and to ensure that the only differences in structure resulted from metal effects in binding of the inhibitor. Crystallographic diffraction data sets for the complexes of Zn-CPA/(I), Ni-CPA/(I) and Hg-CPA/(I), were collected and refined to final R factors of 15.0% (1.7 Å), 15.8% (1.7 Å) and 14.5% (1.8 Å), respectively (Table 2). The resultant Fourier difference maps (*e.g.* Fig. 3) calculated with and without the inhibitor present clearly showed electron density for (I), as well as changes in conformations of active-site residues. The detailed binding of (I) to the active site of native CPA is shown

Table 2. Data measurement and refinement parameters for complexes of BS with native CPA, Hg-CPA and Ni-CPA

	Native	Ni-CPA/(I)	Hg-CPA/(I)
Detector	CPA/(I)	R-AXIS-IIc	FAST
Independent reflections	21267	23403	22064
$R_{\text{merge}}/R_{\text{sym}}$ (%)	6.12	5.14	6.04
No. of refinement cycles	47	25	34
No. of water molecules	203	203	216
R.m.s. deviation (σ -target)			
Bond lengths	0.011 (0.015)	0.011 (0.015)	0.014 (0.015)
Average w ($^{\circ}$)	1.9 (2.5)	1.9 (2.5)	2.3 (2.5)
Final r.m.s. coordinate shifts	0.009	0.007	0.009
Resolution (\AA) (cutoff on F)	5.00–1.70 (2.5 σ)	5.00–1.70 (2.5 σ)	5.00–1.80 (2 σ)
Final R factor (%)	15.0	15.8	14.5

in Fig. 4 where the active site is superimposed on the corresponding region of the uncomplexed native enzyme. As shown in this superposition, (I) displaces the metal-bound water and binds in the position usually occupied by bound analogues and inhibitors (Shoham, Christianson *et al.*, 1988; Christianson & Lipscomb, 1989), causing the commonly observed conformational changes associated with inhibitor/analogue binding. The main features of this structure are in agreement with a recently published lower resolution structure of CPA/(I) (Mangani *et al.*, 1992a), although some structural details remain different in the two structures and may be a product of the different resolution limits involved in the two studies. In the current enzyme–inhibitor model the terminal carboxylate (B-carboxylate) forms a salt bridge with the guanidinium group of Arg145 and hydrogen bonds with Tyr248 and Asn144. Tyr248 is rotated into a 'down' position allowing better interactions between it and the bound inhibitor, and blocking off the active site from solvent. This large conformational change of Tyr248 is tied to a distinct conformational change of the peptide chain in the region of residues 246–250.

Of principle interest is the second carboxylate group (A-carboxylate) of (I) which displaces the water in the apical ligand position and binds to the zinc ion as a nearly symmetrical bidentate ligand. This mode of binding is energetically favorable, yet it was not the expected result since in the analogous complex of (I) with thermolysin the A-carboxylate of the inhibitor binds to the metal as a monodentate ligand (Bolognesi & Matthews, 1979). In the present CPA/(I) complex, the zinc ion moves about 0.4 \AA from its original position towards the bound inhibitor and away from its ligands. One should note that in addition to binding the metal, the A-carboxylate also forms close contacts with both Glu270 (the tetrad 'base') and Arg127 [the tetrad 'electrophile' (Christianson & Lipscomb, 1989; Feinberg *et al.*, 1993)]. These potentially important catalytic groups are positioned symmetrically on either side of the carboxylate group, where $N^{\eta 1}$ of Arg127 is 2.6 \AA from one of the carboxylate O atoms (O1) and $O^{\epsilon 1}$ of Glu270 is 2.6 \AA from the other carboxylate O atom (O2). This arrangement suggests that there

is a considerable interaction between the inhibitor carboxylate O atom (O2) and Glu270. The hydrogen bonds implicit in the enzyme–inhibitor structure would contribute further stability to this complex. Such interactions between the A-carboxylate and the functional groups of the active site, and the strong bidentate interactions between the inhibitor and the metal may account for the potent inhibitory properties of (I) and may be relevant for other carboxylate inhibitors.

Comparable structural analyses have been performed with complexes of (I) and the other metallo-CPA derivatives. The final structures of Zn-CPA/(I), Ni-CPA/(I) and Hg-CPA/(I) have been compared and indicated a high degree of similarity. The distances between the main functional groups in each of the three structures are listed in Table 3. There appear to be no significant changes in the binding geometry of (I) when the active-site metal is changed. An exception is Arg127 in the mercury derivative. In this instance, the side chain of Arg127 appears to adopt a conformation similar to that found in the native (unbound) structure. In this mercury-derivatized enzyme structure the interaction of the inhibitor carboxylate O atom with Arg127 $N^{\eta 1}$ is replaced by a hydrogen bond to a water molecule (2.6 \AA), which in turn forms a hydrogen bond to the N^{ϵ} (2.2 \AA) and $N^{\eta 1}$ (2.2 \AA) of Arg127. While there are some small structural differences in the three active-site structures, the bound inhibitor generally binds in the same location and forms similar interactions independent of the active-site metal. The three metals bind the A-carboxylate of the inhibitor in the previously described bidentate fashion. Even the metal–carboxylate distances are comparable, if one considers the differences in ionic radii of the three metals. One conclusion, therefore, is that the general mode of binding of (I) is not directly dependent on the specific metal present in the active site. Since benzyl succinate resembles a whole family of inhibitors and analogues these results suggest that the mode of substrate binding may not be dependent on the specific metal at the active site, and that the differences in observed activities of various metallo-CPA derivatives are the result of the relative catalytic competence of a given metal and not from altered binding phenomena.

Complexes of native CPA with keto methylene analogues

In addition to using inhibitors, one may also study the binding characteristics of the active site of an enzyme by examining the complexes of an enzyme with non-reactive reaction coordinate analogues. Among such complexes of CPA that have been examined to date are those with Gly-Tyr (Lipscomb *et al.*, 1968; Rees & Lipscomb, 1983) and several amino-acid, aldehyde, ketone, phosphonate and phosphoramidate analogues (Christianson & Lipscomb, 1985a,b, 1986a,b, 1987; Christianson *et al.*, 1987, 1989; Kim & Lipscomb, 1991; Mangani

et al., 1992a,b; Mangani & Orioli, 1992). Interesting structural changes occur to CPA active-site residues upon interaction with these compounds, and many details regarding substrate interactions with the enzyme have been deduced from structural analyses of these complexes. A drawback in these studies lies in the fact that all these substrate-like molecules seem to behave abnormally in their interaction with the enzyme as reflected, for example, in deviations from Michaelis-Menten kinetics.

In an attempt to avoid these problems, we designed a new series of substrate analogues for use in crystal structure analysis. This is the series of di-, tri- and tetrapeptides containing one pseudo-peptide bond located in place of the scissile peptide bond (Ewenson, Cohen-Suissa *et al.*, 1988; Ewenson, Laufer *et al.*, 1988; Shoham, Oren, Ewenson & Gilon, 1988). The pseudo-peptide bond is a keto-methylene (KM) bond, in which CH_2 is substituted for the NH moiety. The advantage of these analogues over the previously described compounds is their similarity to natural peptides, both in residue type and conformation. In addition, these analogues are resistant to cleavage in the active site of CPA because of the strength of the $\text{CO}-\text{C}$ bond. These analogues have the general structure $X-(R,S)\text{Phe-}\psi-(R,S)\text{Phe-OH}$ [ψ represents a keto-methylene bond ($-\text{CO}-\text{CH}_2-$) rather than the normal peptide bond ($-\text{CO}-\text{NH}-$)], where X is a moiety with varying size and hydrophobicity.

Several such analogues [Ac-Phe- ψ -PheOH, (II); pGlu-Phe- ψ -PheOH, (III); Boc-Phe- ψ -PheOH, (IV); Bz-Phe- ψ -PheOH, (V); BocPhe-Phe- ψ -PheOH, (VI); NH_2 -Ala-Phe- ψ -PheOH, (VII)] were prepared, in order to mimic the blocked dipeptide PhePheOH, the blocked tripeptide PhePhePheOH and the unblocked tripeptide AlaPhePheOH, respectively, all of which are good natural substrates of CPA. These pseudo-peptides were examined kinetically and were found to bind to the enzyme with high affinity and were found to be potent competitive inhibitors (Shoham, Christianson *et al.*, 1988, Shoham, Oren *et al.*, 1988; Behar *et al.*, manuscript in preparation). The observed K_i values (measured for both peptidase and esterase activities) are well within the submicromolar range (Table 4). Please note that the KM inhibitors have been synthesized and examined as a stereoisomeric mixture and the actual kinetic values for the particular active species (which is found in the crystal structure complex) is hence significantly smaller. Specific K_i values observed appear to be largely dependent on the size and hydrophobicity of the blocking group (X), an experimental result that is very important for the design of second generation inhibitors.

Cross-linked CPA crystals were incubated with analogues (II)–(VII) yielding the corresponding crystal complexes. We analyzed structures of the CPA complexes of (II), (IV) and (V), for which the crystals were found to be isomorphous with crystals of native CPA and

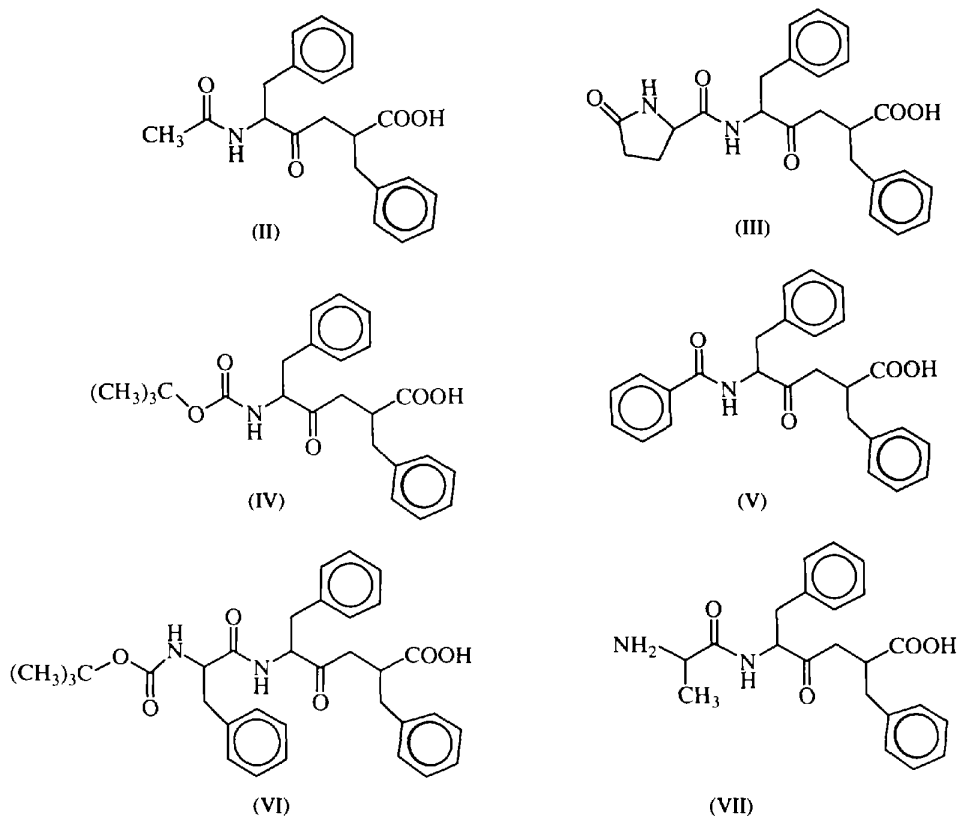
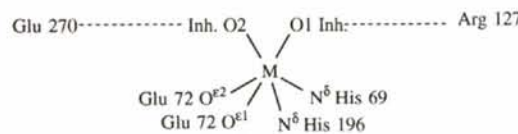


Table 3. Selected active-site distances (Å) in the complexes of native CPA, Hg-CPA and Ni-CPA with L-benzylsuccinate



		Native CPA/(I)	Ni-CPA/(I)	Hg-CPA/(I)
al	O1	2.36	2.35	2.64
al	O2	2.39	2.22	2.43
Glu270	O2	2.61	2.72	2.73
Glu270	O2	3.41	3.52	2.65
Arg127	O1	2.61	2.77	5.63
Arg127	O1	—	—	2.63-(O)-2.18
Arg127	O1	—	—	2.63-(O)-2.20
His69	Metal	2.21	2.12	2.37
Glu72	Metal	1.98	2.20	2.08
Glu72	Metal	2.73	2.48	2.56
His196	Metal	2.14	2.35	2.07

for which high-resolution data were collected. The structures of CPA/(II), CPA/(IV) and CPA/(V) were refined and converged to final *R* factors of 14.8% (1.7 Å), 23.6% (1.75 Å), and 15.5% (1.7 Å), respectively (Table 5). A more thorough structural discussion of the CPA/

Table 4. Inhibition parameters for CPA (peptidase and esterase activities) with keto-methylene inhibitors

Peptidase activity was measured by inhibiting the hydrolysis of dansyl-Gly-L-Trp (2×10^{-5} to 2×10^{-6} M), at 0.5 M NaCl, 0.05 M Tris/HCl pH = 7.5, [CPA] = 1×10^{-8} M. Esterase activity was measured by inhibiting the hydrolysis of *o*-(*trans*-*p*-chlorocinnamoyl)-L-β-phenyllactate (1×10^{-5} to 8×10^{-5} M), at 0.5 M NaCl, 0.5 M Tris/HCl pH = 7.5, [CPA] = 7×10^{-10} M.

Inhibitor	<i>K_i</i> (Peptidase) (M)	<i>K_i</i> (Esterase) (M)
Ac-(<i>R,S</i>)Phe-ψ-(CO-CH ₂)-(R,S)Phe-OH	1.2×10^{-6}	1.6×10^{-6}
pGlu-(<i>R,S</i>)Phe-ψ-(CO-CH ₂)-(R,S)Phe-OH	4.7×10^{-7}	8.3×10^{-7}
Boc-(<i>R,S</i>)Phe-ψ-(CO-CH ₂)-(R,S)Phe-OH	5.1×10^{-7}	5.0×10^{-7}
Bz-(<i>R,S</i>)Phe-ψ-(CO-CH ₂)-(R,S)Phe-OH	8.4×10^{-8}	6.4×10^{-8}
Boc-(<i>S</i>)Phe-(<i>R,S</i>)Phe-ψ-(CO-CH ₂)-(R,S)Phe-OH	7.5×10^{-8}	6.3×10^{-8}

(IV) complex has been presented elsewhere (Shoham, Christianson *et al.*, 1988). In all three cases the initial difference maps indicated the binding of the analogue in the active site and apparent removal of the zinc-bound water (Fig. 5). In all cases the analogue is interacting directly with the zinc and causes the typical conformational changes in the active-site residues. Since the analogues are bound statistically to a fraction of the enzyme molecules in the crystal [with total occupancy of

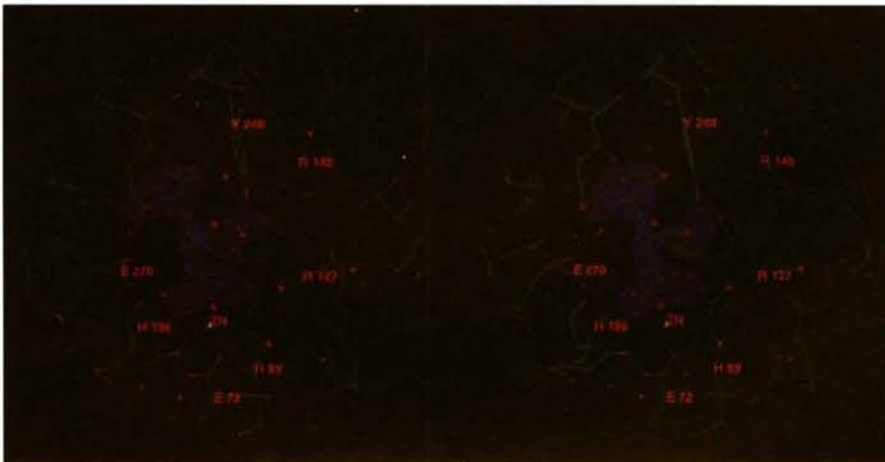


Fig. 3. Difference Fourier map of the complex of CPA/(I) (active site). The map was calculated with $[F_{\text{obs}} - F_{\text{calc}}]$ Fourier coefficients. For this calculation, the final model of CPA/(I) was used, but with the benzyl succinate molecule removed. Contouring of the electron density (in blue) is carried out at 3.5σ .

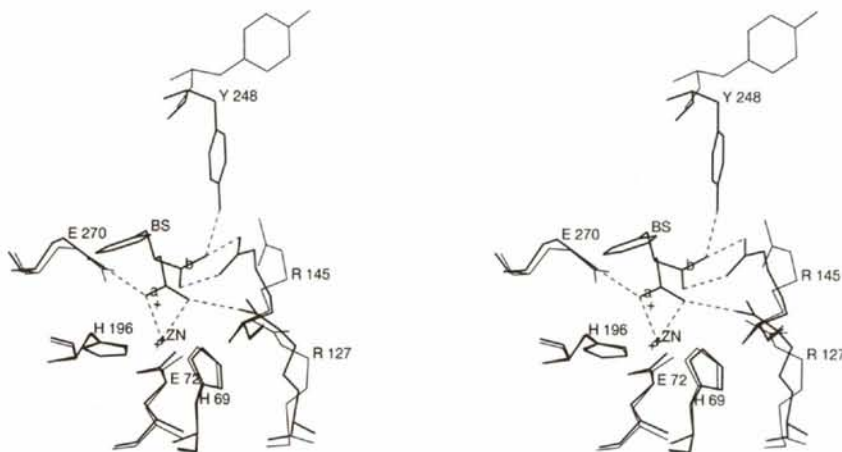


Fig. 4. Native CPA (thin lines) versus the complex of CPA/(I) (thick lines). Dotted lines represent interactions in the complex.

Table 5. *Data measurement and refinement parameters for CPA complexed with keto-methylene (II) and (V)*

	CPA/(II)	CPA/(V)
Independent reflections	24065	26718
$R_{\text{merge}}/R_{\text{sym}}$ (%)	5.87	3.01
No. of cycles	38	51
No. of water molecules	211	200
R.m.s. deviation (σ -target)		
Bond lengths	0.012 (0.015)	0.013 (0.015)
Average w ($^{\circ}$)	2.0 (2.5)	2.2 (2.5)
Final r.m.s. coordinate shifts	0.018	0.012
Resolution (\AA) (cutoff on F)	5.0–1.7 (2.5 σ)	5.0–1.7 (2.5 σ)
Final R factor (%)	14.8	15.5

0.5–0.8 (50–80%)] it is possible to compare the conformations of the active-site residues before and after binding. For example, in the crystals of the CPA/(V) complex approximately half of the CPA molecules have bound analogue while the other half of the molecules have no analogue bound. We were able to resolve the two conformations involved and hence to determine and

refine in parallel the structures of the complexed and uncomplexed native enzyme within the same crystal structure (Fig. 6). Most of the conformational changes observed upon binding of the keto-methylene analogues are those observed with bound inhibitors and have been discussed in detail elsewhere (Shoham, Christianson *et al.*, 1988; Christianson & Lipscomb, 1989). Most of the active-site residues, including the three arginines (71, 127 and 145), Tyr248 and Glu270, have moved significantly from their positions in the native enzyme in order to accommodate the analogue.

The areas of primary interest are obviously the zinc-binding pocket and the metal-analogue interface. The electron-density difference map around the keto-methylene bond shows well defined bifurcated electron density corresponding to a hydrated ketone: the species observed bound to the enzyme is the tetrahedral hydrated form of the carbonyl, a mimic of the proposed tetrahedral intermediate formed as an intermediate in catalysis. This

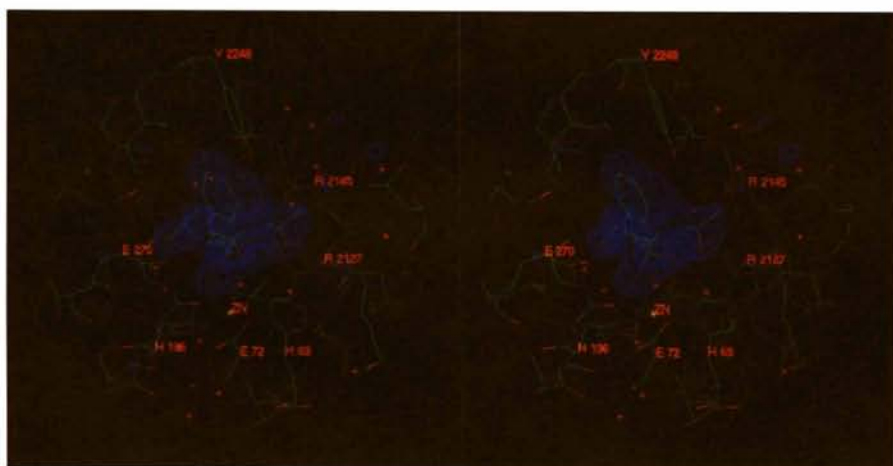


Fig. 5. Difference Fourier map of the active site of CPA/(II). The map was calculated with $[F_{\text{obs}} - F_{\text{calc}}]$ Fourier coefficients. For this calculation, the final model of CPA/(II) was used, but with the molecule of (II) removed. Contouring of the electron density (in blue) is carried out at 3.0σ .

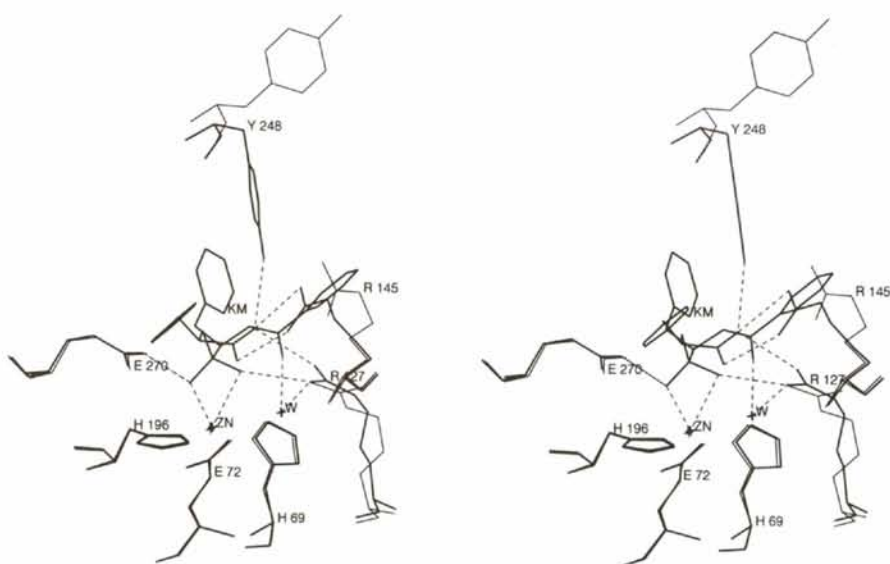


Fig. 6. Active site of CPA showing binding of benzoyl-Phe- ψ -Phe (V) to CPA (thick lines) relative to native CPA (thin lines). Dashed lines represent hydrogen bonds or other favorable interactions.

Table 6. Selected active-site distances (Å) in the complexes of native CPA with keto-methylene inhibitors (II), (IV) and (V)

		CPA/(II)	CPA/(IV)	CPA/(V)
Zn	O1	3.08	2.13	2.62
Zn	O2	2.18	2.62	2.20
O ^{ε1} Glu270	O2	3.23	2.45	2.92
O ^{ε2} Glu270	O2	2.69	2.56	2.48
N ^{η1} Arg127	O1	2.99	3.26	3.02
N ^{η2} Arg127	O1	3.09	—	3.51
N ^δ His69	Zn	2.14	2.15	2.14
O ^{ε1} Glu72	Zn	2.10	2.11	2.17
O ^{ε2} Glu72	Zn	2.44	2.53	2.53
N ^δ His196	Zn	2.08	2.30	2.09

result was initially not expected as this particular ketone does not possess an exceptionally electrophilic carbonyl, and therefore was not expected to exist in aqueous solution in hydrated form (Shoham, Christianson *et al.*, 1988). In our structure though, this enzyme-inhibitor complex appears as a stable species which resembles a structure along the reaction coordinate and not a reactant or a product. The results obtained from this and other keto-methylene pseudopeptides strongly support the notion that after initial binding of analogue to the enzyme the ketonic carbonyl is attacked by a water molecule (presumably the zinc-bound water) resulting in a stable *gem*-diol. Since the scissile peptide bond has been replaced by a less reactive one, cleavage cannot take place, and the inhibitor remains trapped in the enzyme. The two hydrate O atoms are arranged above the zinc ion with typical zinc-O atom distances of 2.2 and 2.6 Å. Interestingly, the *gem*-diolate appears to be further stabilized by close interactions with the two other active-site residues. One hydrate O atom (O1) receives a hydrogen bond from Arg127 and the other hydrate O atom (O2) makes a hydrogen bond to Glu270.

Structural analyses of the complexes of CPA with analogues (II), (IV) and (V) revealed a similar arrangement of the *gem*-diolate, the zinc ion and the active-site catalytic residues. The three structures are shown in Fig. 7 and the relevant bond distances are listed in Table 6. In all three cases the resulting *gem*-diolate interacts with the zinc ion and with residues Arg127 and Glu270. For analogues (II) and (V) two such interactions are present between each of these residues and the corresponding hydrate O atoms (Table 6). Such strong interactions may account for part of the tight binding of these inhibitors. If we consider these resultant *gem*-diolates as reaction intermediate analogues, then these interactions suggest a possible role of the zinc ion and active-site residues in the stabilization of a true catalytic intermediate.

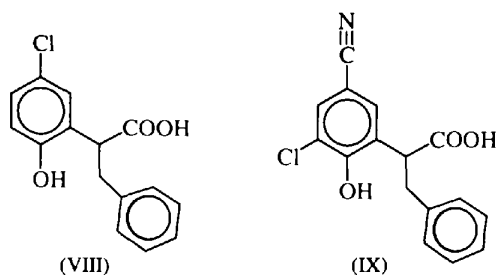
The detailed structural information on the complexes of the keto-methylene analogues with CPA additionally gives insights into how different blocking groups interact

with the extended active site of the enzyme. Although not discussed above, the analogue-enzyme interactions observed in the outer binding cleft (where the X blocking group binds) (Abramowitz *et al.*, 1967) could explain, at least in part, the dramatic increase in inhibition from analogue (II) to (V) (Table 4) on the basis of specific interactions. As discussed elsewhere (Feinberg *et al.*, 1993), information gleaned about interactions outside the specificity pocket can often be exploited to make a drug more specific for one member of a class of enzymes. Thus, while many zinc exoproteinases may have similar specificity pockets and active sites, they generally differ in the regions outside the active site. These differences can be used to render a given inhibitor highly specific for one enzyme, while having little effect on other related enzymes. This concept agrees well with the general idea outlined above suggesting the combination of zinc-binding component and substrate-specificity component(s) in the rational design of high-affinity inhibitors for a specific zinc proteinase.

Complexes of native CPA with phenolate inhibitors

A novel class of inhibitors displaying tight binding to CPA are based on phenol derivatives. These phenol inhibitors show competitive inhibition in the micromolar range and it has been suggested that they bind to the active-site zinc *via* direct interaction of the phenol hydroxyl group (Mock & Tsay, 1986, 1988; Mock, Freeman & Aksamawati, 1993). The phenol ring can be modified with various substituents which affect the inhibition constant (Mock *et al.*, 1993). Two such inhibitors were used recently for the examination of zinc-phenol interactions. The inhibitors are α -(5-chloro-2-hydroxyphenyl)benzenepropanoic acid [(VIII)], and α -(3-chloro-5-cyano-2-hydroxyphenyl)benzenepropanoic acid [(IX)]. These two inhibitors have been introduced into CPA crystals and the resulting complexes were analyzed by X-ray crystallography at high resolution. Cross-linked crystals of native CPA were soaked in solutions containing increasing concentrations of each inhibitor, until a maximum concentration of 1 mM was attained. The crystals were then allowed to soak for at least one week. One crystal from each inhibitor solution was chosen for data collection on a Rigaku R-Axis IIc imaging-plate area detector (Shibata, 1990; Sato *et al.*, 1992) coupled to a Rigaku RU-300 rotating-anode source with a mirror-mirror optical focusing system. Data-collection parameters for the CPA/(VIII) and CPA/(IX) complexes, as obtained from the Rigaku original processing software (*PROCESS*, Sato *et al.*, 1992), are summarized in Table 7. Initial difference maps using native CPA showed very clear density for both inhibitors, as well as the changes which occur in the active-site residues (Fig. 8). While most of the changes were typical of those seen in the structures of other inhibitors, one notable exception was the

repositioning of the side chains of Glu270 and Thr268. Once the inhibitors were fit and all the appropriate side chains modified, several cycles of restrained least-squares refinement (Hendrickson & Konert, 1981) were performed (Table 7). The final structure of the complex between CPA and (IX), is shown with the native enzyme in Fig. 9. The structures of (VIII) and (IX) bound to the active site of CPA have been compared and shown to be very similar. The small differences in the active-site positions of the inhibitors are presumably due to the different arrangements of the substituents on the hydroxyphenyl ring. Active-site distances for both CPA complexes are listed in Table 8.



Since the pK_a of the phenolic O atom of (IX) is between 7.1 and 7.2 Å, it is certainly reasonable to assume that the inhibitor is bound in the deprotonated state to the metal ion. Stabilization of the phenolic anion would be consistent with one of the roles that has been generally proposed for the zinc ion in CPA (Feinberg *et al.*, 1993), which is to stabilize the evolving negative charge on the carbonyl O atom of a substrate during catalysis. Since the pattern of binding for (VIII) is nearly identical to that observed for (IX), one can assume that the former has also bound in its phenolic state. This is consistent with previous proposals (Mock & Tsay, 1986) regarding the protonation state of the bound form of the inhibitor. A more indirect indication of the deprotonation of the inhibitor upon binding involves the unique changes in the conformations of the side chains of Glu270 and Thr268. The only apparent hydrogen bond that the carboxylate group of Glu270 forms is to the O^γ of Thr268. It is unlikely that such an interaction would be sufficient to stabilize a full negative charge on Glu270 if it remained unprotonated. If, on the other hand, Glu270 were protonated, then the resulting neutral side chain could be quite stable in the environment observed in the inhibitor–enzyme complex. An increase in the pK_a of Glu270 would also be expected because of the hydrophobic nature of that region of the active site following positioning of the phenol ring.

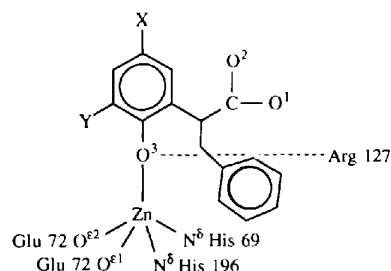
Since these inhibitors do not undergo covalent chemical modification upon binding as do the keto-methylene inhibitors, they are closer to being substrate analogues, rather than intermediate or transition-state analogues. If so, one might be tempted to propose that the structures of the inhibitors bound to the active site should be

Table 7. *Data measurement and refinement parameters for CPA complexed with the phenolate inhibitors (VIII) and (IX)*

	CPA/(VIII)	CPA/(IX)
Independent reflections	23759	33599
$R_{\text{merge}}/R_{\text{sym}}$ (%)	5.37	5.25
No. of cycles	24	30
No. of water molecules	195	204
R.m.s. deviation (σ -target)		
Bond lengths	0.014 (0.015)	0.014 (0.015)
Average w ($^\circ$)	2.4 (2.5)	2.6 (2.5)
Final r.m.s. coordinate shifts	0.009	0.009
Resolution (Å) (cutoff on F)	5.0–1.75 (2.5 σ)	5.0–1.60 (3.0 σ)
Final R factor (%)	14.2	15.2

Table 8. *Selected active-site distances (Å) in the complexes of native CPA with the phenolate inhibitors (VIII) and (IX)*

For inhibitor (VIII) $X = \text{Cl}$, $Y = \text{H}$; for inhibitor (IX) $X = \text{CN}$, $Y = \text{Cl}$.



		CPA/(VIII)	CPA/(IX)
Zn	O3	2.0	1.9
N ^η 1 Arg127	O1	3.2	3.5
N ^η 2 Arg 127	O3	3.0	3.2
N ^δ 2 Asn144	O1	2.9	2.9
N ^η 1 Arg145	O1	2.7	2.8
N ^η 2 Arg145	O2	2.7	2.8
O ^η Tyr248	O2	2.7	2.6
N ^δ His69	Zn	2.1	2.1
O ^ε 1 Glu72	Zn	2.1	2.0
O ^ε 2 Glu72	Zn	2.8	2.8
N ^δ His196	Zn	2.1	2.1

good models for the Michaelis–Menten complex. This proposal would not be very accurate, however, for the following reasons. The K_m of typical substrates lies in the millimolar range (Coleman & Vallee, 1962), while the K_i for these inhibitors falls in the micromolar range. This is presumably due, in part, to the increased affinity of the phenolate O atom for the metal ion, relative to the (formally) uncharged carbonyl group of a substrate. In addition to this difference, the position adopted by the O atom of the phenolate group relative to the metal ion and other side chains is directly coupled to the position assumed by the bulky phenol ring and its substituents. Finally, the water molecule which should be poised to attack a substrate or a good mimic is not apparent in the immediate vicinity of the relevant part of the inhibitor. Given these differences between the inhibitors and a true substrate mimic, proposals about the nature of the pre-catalytic complex (Christianson & Lipscomb, 1989) are neither confirmed nor contradicted by the structures

presented here. Despite these differences, these inhibitors clearly represent useful templates for the construction of novel inhibitors of CPA and related carboxypeptidases. The delocalization of charge in the phenol ring of these inhibitors offers a feature not present in other inhibitors. This feature presumably makes a significant contribution to the relatively high affinity these molecules exhibit for CPA and TLN (Mock & Aksamawati, 1994). This could simply be because of the greater propensity of the hydroxyl group to lose a proton, or because of electronic interaction between the zinc and the phenolate ring, or a combination of both.

Another interesting observation in the two structures presented here is the increase in the unidentate nature of the interaction between Glu72 and the zinc ion. In native CPA (Greenblatt, Feinberg & Shoham, unpublished results) both O atoms of the carboxylate group of Glu72 are equidistant from the zinc. In structures of CPA with keto-methylene inhibitors bound in the active site (Feinberg *et al.*, 1993) the interaction is more asymmetric. These inhibitors were refined at 0.5 occupancy. In the current structures, where the occupancy is estimated to be 0.8 for both inhibitor structures, the asymmetry is even greater. This trend would imply that binding

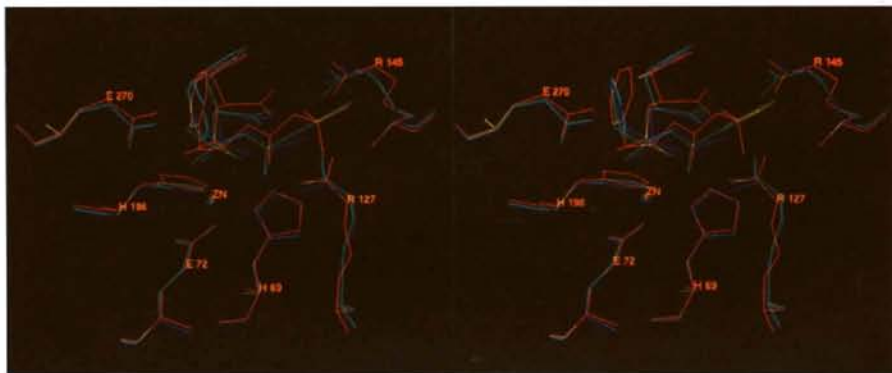


Fig. 7. A comparison of keto-methylene inhibitors bound to CPA: acetyl-Phe- ψ -Phe [(II), blue], BOC-Phe- ψ -Phe [(IV), red] and benzoyl-Phe- ψ -Phe [(V), green].

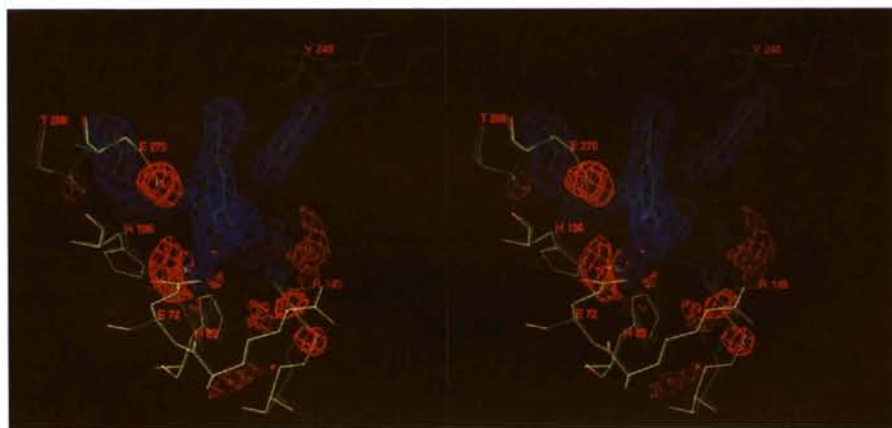


Fig. 8. Difference Fourier (initial) map of the active site of the complex of CPA/(IX). Contouring of the electron density is carried out at 3.5σ (positive, blue, negative, red). Final model of the complex is presented in colors while the superimposed native CPA structure is presented in yellow.

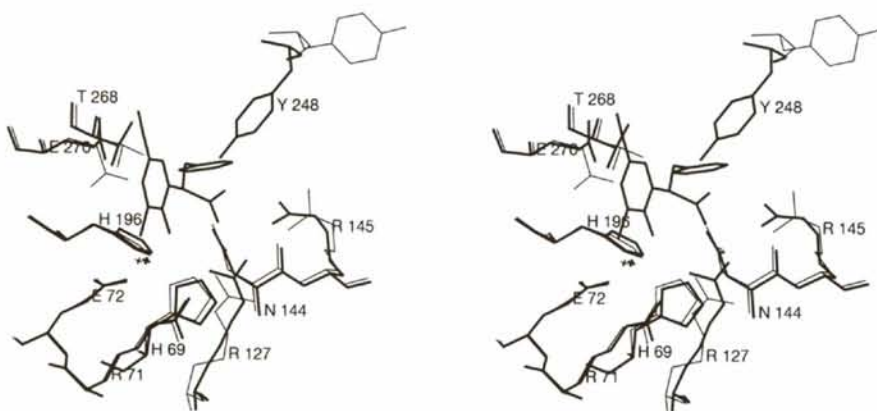


Fig. 9. Stereo comparison between the structures of CPA/(IX) (thick lines) and native CPA (thin lines).

of a substrate or an intermediate affects the interaction between Glu72 and the zinc ion as shown in Table 8 and further discussed below.

Long-range electrostatic interactions of the zinc ion

The program *DelPhi* uses an algorithm which calculates electrostatic potentials of molecules, based on the three-dimensional distribution of charged atoms in and around the molecule (Gilson & Honig, 1987; Gilson, Sharp & Honig, 1988). This algorithm was applied in a number of CPA models in order to evaluate the contribution of long-range electrostatic interactions in the mode of binding of zinc proteinases. Since the enzyme must bind the negatively charged C terminus of a substrate, we wished to investigate what role electrostatics might play in attracting the molecule to the active site, and to what extent, if any, the metal might contribute to this effect.

The calculation was performed on native CPA, in a medium of water, at physiological pH and ionic strength. The resulting electrostatic map (Fig. 10a) showed a prominent concentration of positive electrostatic potential emanating from the active site. In order to estimate the contribution of the zinc ion to the observed potential, the calculation was performed with the zinc removed (apo-CPA), and no other modifications to the charges. In this case, negative electrostatic potential emanates from the active site (Feinberg *et al.*, 1993), suggesting that the zinc ion contributes significantly to the long-range electrostatic attraction of the negatively charged substrate into the active site of the enzyme. It should be noted, however, that the electrostatic potential of this region of the enzyme is very sensitive to the exact protonation state assigned for the two zinc-binding histidines. Given that in the apoenzyme there is a close contact between the side chains of His196 and Glu270 (Fig. 2 above), it may be assumed that this side chain bears a full positive charge. In an extreme case, His69 may also bear a full positive charge in the absence of zinc, as its $N^{\epsilon 2}$ lies within 2.9 Å of Asp142 $O^{\delta 1}$, and its $N^{\delta 1}$ is 3.1 Å away from Glu72 $O^{\epsilon 1}$. When the calculation was repeated with a full charges on both His196 and His69, the long-range distribution of electrostatic potential resembles, at least partially, the potentials obtained for the native enzyme, as shown in Fig. 10(b). In principle, therefore, any long-range electrostatic contribution to substrate binding arising from the metal ion in the active site might possibly be replaced by a full protonation of the two ion-coordinating residues in the apoenzyme. Based on these results, one should be more careful in estimating the magnitude of long-range attraction potential contributed by the zinc ion, since the two active-site histidines could effectively display a charge which is anywhere between these two extreme protonation states. It is thus suggested that the importance of the zinc ion in substrate binding (as reflected in a lack of binding in its absence)

may result only to a limited extent from attracting the substrate to the enzyme.

Another reasonable electrostatic contribution of the zinc ion to substrate binding may result from properly orienting the substrate in the active site. A more detailed investigation of the changes in the electrostatic potential in the active site, even in the extreme case where the two zinc-binding histidines are fully protonated, shows that there are significant differences in the spatial distribution of potential in the substrate-binding region (Fig. 10c). These investigations show that there is a decrease in positive electrostatic potential in the region of the active site where a substrate should bind, a decrease which would affect the ability of apo-CPA to bind substrates or inhibitors. These results would go some way to explaining the observations of Coleman & Vallee (1962) that substrates bound to apo-CPA with somewhat lower affinity than to native CPA, based on K_m values.

Zinc model compounds for the active site of zinc proteinases

The design, preparation, chemical and structural characterization of small molecular models mimicking the metal-binding site of a metalloprotein can contribute invaluable information for the understanding of protein function and structure. Such studies are especially important for the detailed study of the chemical reactivity and the precise geometric parameters of the metal-binding site. Stable model compounds, which are often available in pure form and large quantities, can be effectively used to identify important features of the metal site and clarify coordination geometry. The primary advantage of small molecular models is that their three-dimensional structure can be elucidated at high resolution and their chemical and physical characteristics can be studied directly. Critical properties of the central metal, such as complex stability, ligand lability, overall reactivity, ligand specific pK_a and various spectroscopic parameters, can be measured and assigned in a relatively straightforward and unique fashion.

In addition to contributing to the understanding of structure and function of native proteins, model compounds can clarify the mode of substrate binding and the mechanism of action of proteins. For such studies one attempts to design a model of the protein-ligand complex, the reaction intermediate or the transition state, and use the information gleaned from a structural study in order to explain data observed for the relevant protein system. It should be noted that in these studies it is assumed that the chemical and structural behavior of the metal does not change significantly between the model compounds and the protein environment. This assumption seems reasonable since the fundamental chemistry of a particular metal is not expected to vary significantly in different environments as long as the

electronic state of the metal ion and its first coordination sphere are similar (Karlin, 1993).

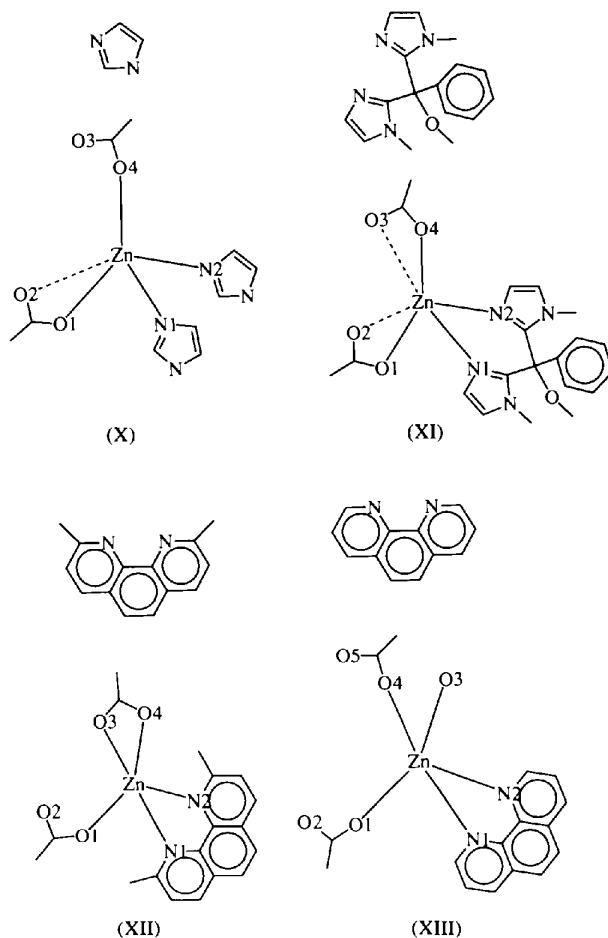
The structural study of model compounds is especially valuable for zinc enzymes because of the poor spectroscopic characteristics of Zn^{2+} ions and the rather limited experimental methods which can be used to characterize the zinc environment and metal behavior. Interesting results have been obtained from molecular design studies [especially carbonic anhydrase (CA) and CPA] which attempted to mimic the zinc-binding site of the native enzyme in order to determine the geometry and chemical characteristics of the enzyme metal-binding site (Wolley, 1975; Sarkar, 1977; Groves & Chambers, 1984; Groves & Olson, 1985; Groves & Baron, 1989; Kimura, 1994). In a similar vein a series of zinc complexes was prepared in our laboratory, focussing on the subgroup of zinc proteinases which has catalytic zinc coordinated to the protein side chains of two histidines, a glutamate and a water molecule (*e.g.* CPA, TLN). Since the zinc ligands in all zinc proteinases are remarkably similar even in those members of the family that share low levels of structural and sequence homologies (Jernigan, Raghunathan & Bahar, 1994), the particular zinc compounds discussed here should be applicable also to the larger family of zinc proteinases.

To mimic the native zinc enzyme we sought zinc model compounds in which the zinc is coordinated to two heterocycle nitrogen ligands, a carboxylate ligand and a water molecule, with an overall coordination number of 4–5 [where the zinc-bound carboxylate (*e.g.* Glu72 in CPA) can contribute one or two liganding sites]. As presented above, in the CPA complexes with carboxylic inhibitors (*e.g.* benzyl-succinate derivatives) and transition-state analogues (*e.g.* keto-methylene derivatives) the coordinated water is exchanged for a carboxylate group in the CPA/(I) complex and a *gem*-diolate group in the CPA/KM complexes. The overall coordination number of the zinc ion in these cases is 4–6 since the groups of both Glu72 and the additional inhibitor ligand(s) appear in those cases in a range of coordination configurations varying from a bidentate ligand to a monodentate ligand. To mimic these enzyme/inhibitor complexes we tried to prepare zinc model compounds in which the zinc metal is coordinated to two heterocycle nitrogen ligands and two carboxylate groups in coordination configurations ranging from 4 to 6. One particular point that we wished to study was whether the zinc coordination geometry in the enzyme is dictated by the constrained geometry of the protein ligands involved, or whether the general coordination geometry preferred by the zinc ion dictates the location of these particular ligands. This question is relevant to various aspects of binding and catalysis of zinc proteinases and in particular has bearing on the general concept of the zinc 'entatic state' which has been proposed in the past (Vallee & Galde, 1984) as a possible explanation for reactivity and efficiency of zinc enzymes.

The different nitrogen ligands employed were varied in their conformation and coordination flexibility, and the resulting zinc coordination geometry was then compared to the corresponding zinc geometries in the enzyme.

Preparation and structural analysis of the model compounds

Presented here are the crystal structures of four zinc complexes which represent a larger set of related zinc proteinase model compounds. Each of these complexes contains a different nitrogen-donating ligand ranging from the most flexible imidazole, to the less flexible BIPhMe [2,2'-bis(1-methylimidazolyl)phenylmethoxymethane] and to the relatively rigid molecules of *o*-phenanthroline and neocuproine (2,9-dimethyl-*o*-phenanthroline). The chemical formulae of these ligands are shown below. The actual complexes for which structural data have been collected are the following: $Zn(\text{acetate})_2(\text{imidazole})_2$ [(X)], $Zn(\text{acetate})_2(\text{BiPhMe}) \cdot 2H_2O$ [(XI)], $Zn(\text{acetate})_2(\text{neocuproine}) \cdot 3H_2O$ [(XII)], and $Zn(\text{acetate})_2(o\text{-phenanthroline}) \cdot H_2O$ [(XIII)]. It should be noted that the structure of the latter zinc complex is part of a larger crystal assembly including (XIII) together with a zinc-

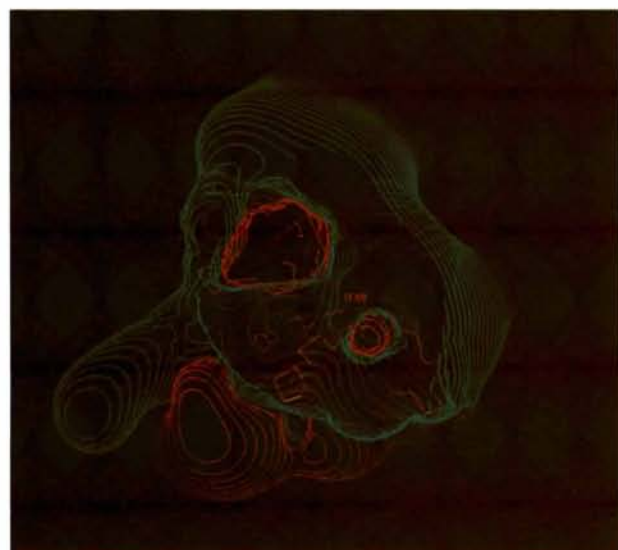


dimer complex $[\text{Zn}_2(\text{acetate})_4(o\text{-phenanthroline})_2]\cdot 4\text{H}_2\text{O}$ [(XIV)]. For the present discussion only complexes (X)–(XIII) will be considered.

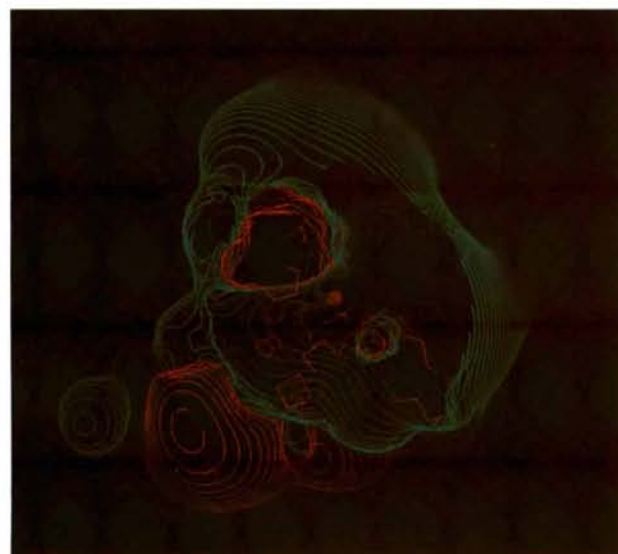
A detailed description of the preparation and crystal structure analysis of these complexes are presented elsewhere (Feinberg *et al.*, 1995, manuscript in preparation). All of the compounds were prepared and crystallized from mixed solutions of $\text{Zn}(\text{acetate})_2$ with the corresponding nitrogen ligand. The crystals obtained were well formed, stable in the X-ray beam and diffracted

to high resolutions. Crystallographic analysis has been performed in the standard procedures (*DIFABS*, Walker & Stuart, 1983; *MITHRIL*, Gilmore, 1984; *SHELXS*, Sheldrick, 1985; *TEXSAN*, Molecular Structure Corporation, 1985) and the resulting parameters are listed in Table 9. Refinement of the structures of (X), (XI), (XII) and (XIII)/(XIV) converged to final *R* factors of 3.4, 4.9, 4.9 and 3.5%, respectively, attesting to the reliability and geometric accuracy of these models.

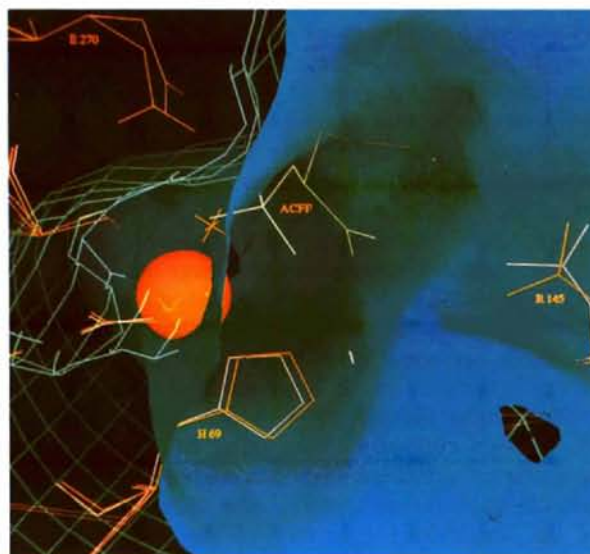
Stereoviews of the final molecular structures of (X)–(XIII) are shown in Fig. 11 and selected bond lengths of these structures are listed and compared in Table 10. All of these mono-zinc complexes contain a core zinc ion with two nitrogen-donating heterocyclic ligands. These are two monodentate imidazole ligands in (X), one bidentate BIPhMe ligand in (XI), one bidentate neocuproine ligand in (XII), and one bidentate *o*-phenanthroline in (XIII). These two ligands represent the two nitrogen ligands in CPA, donated by the imidazole groups of the protein side chains of His69 and His196. In addition to the two nitrogen ligands the first coordination shell of these zinc complexes includes 2–4 oxygen ligands (Table 10), contributed to the complex by the carboxylic groups of two acetic acid molecules [complexes (X)–(XII)] or a combination of two acetic acid molecules and a water molecule [complex (XIII)]. These four oxygen ligands in the model compounds represent, in our view, various combinations of the zinc-bound water, the native zinc ligand Glu72 and the O atoms of a bound inhibitor/analogue.



(a)



(b)



(c)

Fig. 10. (a) Electrostatic potential contours for CPA, calculated using the program *DelPhi*. The contour levels are 0.5 kT e^{-1} (cyan) and -0.5 kT e^{-1} (red), showing quite a large region of positive electrostatic potential emanating from the active site at physiological pH. (b) Electrostatic potential contours for apo-CPA [see (a)], where full compensating charges have been placed on His69 and His196. In such configuration of apo-CPA similar results are observed compared to the long-range potential obtained for native CPA. (c) Close-up of the active site of CPA (orange) and apo-CPA (pink). The zinc ion of native CPA is represented as a CPK sphere. The cyan contour lines represent the 0.5 kT e^{-1} level of native CPA, while the solid contour surface is the same level contour for apo-CPA. The position of a bound inhibitor in native CPA is indicated by compound (II) drawn in white bonds. The results clearly indicate that there is a change in the short-range electrostatic potential of the active site in the area where a substrate or inhibitor would bind.

Table 9. Crystal data and refinement parameters for zinc model compounds (X)–(XIII)

	(X)	(XI)	(XII)	(XIII) + (XIV)
Molecular formula	Zn(Ac) ₂ Im ₂	Zn(Ac) ₂ BIPhMe·2H ₂ O	Zn(Ac) ₂ Neoc·3H ₂ O	Zn(Ac) ₂ O-Phe-H ₂ O/2[Zn ₂ (Ac) ₄ (O-phe) ₂ ·1.4H ₂ O
Content of asymmetric unit	ZnO ₂ N ₄ C ₁₀ H ₁₄	ZnO ₇ N ₄ C ₂₀ H ₂₈	ZnO ₇ N ₂ C ₁₈ H ₂₆	Zn ₂ O ₁₃ N ₄ C ₃₂ H ₃₈
Formula weight	319.63	501.84	447.79	817.43
Space group	<i>P</i> $\bar{1}$	<i>C</i> 2/ <i>c</i>	<i>C</i> 2/ <i>c</i>	<i>I</i> 2/ <i>a</i>
<i>a</i> (Å)	8.077 (1)	18.778 (10)	20.506 (3)	27.353 (4)
<i>b</i> (Å)	11.332 (2)	17.339 (5)	7.956 (1)	12.869 (2)
<i>c</i> (Å)	7.733 (1)	16.361 (15)	26.691 (3)	20.802 (3)
α (°)	99.82 (1)			
β (°)	96.32 (1)	116.66 (7)	108.77	100.02 (2)
γ (°)	92.30 (1)			
<i>V</i> (Å ³)	691.9 (3)	4761 (11)	4123 (2)	7211 (3)
<i>Z</i>	2	8	8	8
<i>D_c</i> (g cm ⁻³)	1.53	1.40	1.44	1.51
Diffractometer	Enraf-Nonius CAD-4	Enraf-Nonius CAD-4	Enraf-Nonius CAD-4	Philips PW1100/20
λ	Cu <i>K</i> α	Cu <i>K</i> α	Cu <i>K</i> α	Mo <i>K</i> α
2 θ max (°)	130	120	120	50
Unique reflections	2250 [<i>I_o</i> > 3 σ (<i>I_o</i>)]	2627 [<i>I_o</i> > 2 σ (<i>I_o</i>)]	2576 [<i>I_o</i> > 2 σ (<i>I_o</i>)]	4855 [<i>I_o</i> > 3 σ (<i>I_o</i>)]
Refined parameters	172	289	279	460
<i>R</i> (%)	3.4	4.9	4.9	3.5
<i>wR</i> (%)	6.4	6.6	7.3	5.1

As can be seen in the three-dimensional structure of the model compounds (Figs 11a–11d) all the carboxylic groups involved in the coordination shell of the zinc complexes interact with the zinc ion in the *syn* configuration (Glusker, 1991; Christianson, 1991). However, the corresponding zinc–oxygen bond lengths (Table 10) indicate that the carboxylic ligands of these complexes use a range of coordination modes for the zinc varying from a clear monodentate coordination mode to a symmetrical bidentate coordination mode (also termed ‘direct’ carboxylate–metal coordination; Glusker, 1991). The shortest distance between a zinc ion and a carboxylic O atom observed in the model complexes is 1.91 Å while the longest corresponding distance is 3.23 Å. For the purpose of the current discussion we will arbitrarily define a zinc–oxygen interaction which is shorter than 2.4 Å as a ‘full’ Zn–O coordination, zinc–oxygen in-

teraction which is in the range of 2.4–2.7 Å as a ‘half’ Zn–O coordination, and zinc–oxygen interaction which is longer than 2.7 Å as a ‘weak’ or a ‘not-significant’ Zn–O coordination. With these definitions one can then examine the overall coordination number of the zinc ion in respect to the oxygen-donating ligands. In complex (X) (Fig. 11a) one of the carboxylate ligands contributes 1.5 coordination sites while the other carboxylate ligand contributes only a single coordination site (total of 2.5 coordination sites). In complex (XI) (Fig. 11b) each carboxylate ligand contributes 1.5 coordination sites (total of three coordination sites). In complex (XII) (Fig. 11c) one of the carboxylate ligands contributes only a single coordination site while the other carboxylate ligand contributes two coordination sites (total of three coordination sites). In complex (XIII) (Fig. 11d) each of the carboxylate ligands contributes only a single coordination site and the bound water molecule contributes an additional coordination site (total of three coordination

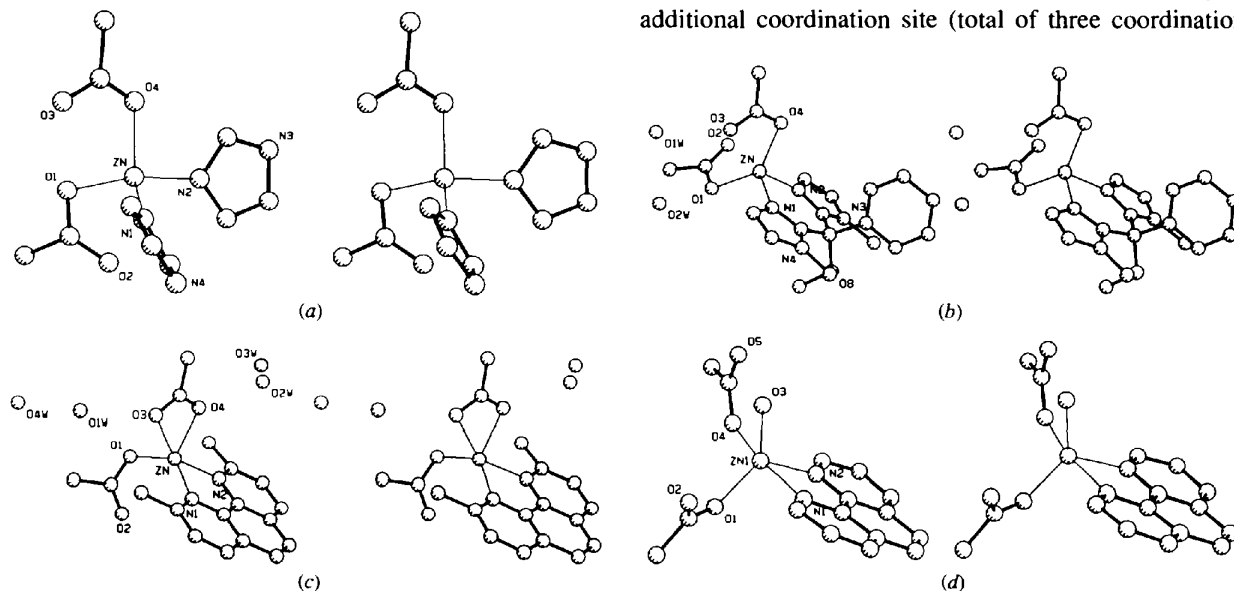


Fig. 11. Stereoview of the final crystal structures of zinc model compounds (X)–(XIII) (PLUTO, Motherwell & Clegg, 1978).

Table 10. Zinc–ligand distances (Å) in zinc model compounds and CPA complexes

In the structure of CPA and its complexes, N¹ corresponds to N^δ(His69), N² corresponds to N^δ(His196), O¹ corresponds to O^{ε1}(Glu72), O² corresponds to O^{ε2}(Glu72), O³ and O⁴ correspond to the inhibitor O atoms liganded to the zinc ion (or water ligand, as indicated).

	N ¹	N ²	O ¹	O ²	O ³	O ⁴
(X)	2.00	2.01	1.99	2.66	—	1.96
(XI)	2.02	2.01	2.00	2.49	2.47	2.06
(XII)	2.06	2.09	1.91	—	2.36	2.08
(XIII)	2.15	2.10	1.95	—	2.02 (H ₂ O)	2.07
Native CPA	2.00	2.08	2.30	2.32	1.95 (H ₂ O)	—
CPA/(I)	2.21	2.14	1.98	—	2.36	2.39
CPA/(II)	2.14	2.08	2.10	2.44	—	2.18
CPA/(V)	2.14	2.09	2.17	2.53	2.62	2.20

sites). Thus, the overall coordination number of the zinc ion in each of these model complexes is 4.5–5 and the overall geometry ranges from a distorted trigonal bipyramid (tbp) to a distorted octahedron.

The four zinc model structures can be readily superimposed. The best superposition of the four structures is obtained when the least-squares fit is performed on the basis of the zinc ion and the two coordinating N atoms of each complex (Fig. 12). This overlap demonstrates that the six coordination sites around the central metal (two sites for the N atoms and four sites for the O atoms) are generally fixed relative to each other in the coordination sphere of the zinc ion. It is noteworthy that although the oxygen ligands in the model compounds differ in their detailed structure around the zinc ion, they generally form similar coordination patterns in terms of both the overall number and spatial distribution of the coordination sites. These results indicate that, at least in small-molecule complexes, the zinc ion may be flexible in terms of the type of ligands with which it reacts and the individual nature of interaction of each ligand with it; however, the overall preferred coordination number and coordination geometry is relatively fixed. This conclusion is not trivial for the series of model compounds presented above if one considers the significant differences in the chemical nature, size and conformational flexibility of the heterocyclic nitrogen ligands involved. Such conclusion may thus have important implications for coordination preferences of zinc ions in proteins.

Comparison of zinc coordination in model compounds and CPA

The zinc–ligand interactions in four of the CPA structures presented above are listed in Table 10 in order to compare the zinc coordination in the model compounds discussed with both native CPA and inhibitor-bound CPA. In the CPA structures it is noted that the carboxylic group of the Glu72 side chain can interact with the zinc ion in either symmetrical bidentate fashion (native CPA), as monodentate only [CPA/(I) complex], or somewhere in between these extremes as a non-symmetrical bidentate ligand [CPA/(II) and CPA/(V) complexes]. According to the simplistic definitions for the 'degree of zinc coordination' outlined above, the Glu72 carboxylate contributes in these cases 2, 1 and 1.5 coordination sites to the zinc ion, respectively. Following similar rationale, the additional, non-protein, ligand in the coordination sphere of CPA (water molecule, bound inhibitor or TS analogue) can interact with the zinc ion as a monodentate ligand [CPA native, CPA/(II) complex], as symmetrical bidentate ligand [CPA/(I) complex], or as a non-symmetrical bidentate ligand [CPA/(V)]. Here again, the assigned 'degree of zinc coordination' is 1, 2 and 1.5, respectively. Considering the oxygen-donating ligands and their coordination mode, one can find close similarities between model compounds (XII) and (XIII), and the CPA/(I) complex, between model compound (X) and the CPA/(II) complex, and between model compound (XI) and the CPA/(V) complex. Moreover, as in the case of the model compounds the overall coordination number of the zinc complex remains at the narrow range of 4.5–5, indicating that the coordination number (and geometry) of zinc in CPA is similar to that of zinc in small molecule compounds with similar ligands.

A related study of zinc model compounds (Horrocks, Ishley, Holmquist & Thompson, 1980; Horrocks, Ishley & Whittle, 1982*a,b*) has been carried out with a series of zinc complexes of the type Zn(RCOO)₂(RIm)₂ (R = alkyl group, Im = imidazole). In these studies it was reported that the zinc model complexes were crystallized with coordination number of 4 (where similar complexes of cobalt display coordination numbers of 4 and 6). On the basis of these results it was suggested that the free

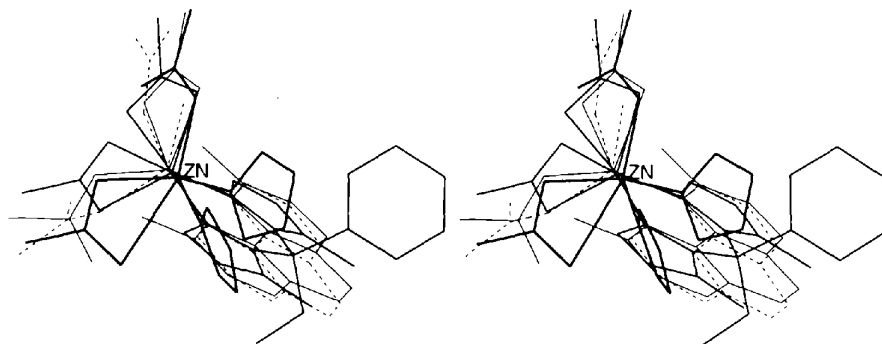


Fig. 12. Superposition of the final structures of zinc model compounds (X)–(XIII).

energy difference between 4- and 6-coordination zinc complexes of this type is relatively small and that the actual structure adopted by the zinc ion will depend upon crystal-packing forces. Our results show that the degree of zinc coordination in zinc complexes of this type (imidazole and carboxylate ligands only) is in the range of 4.5–5. Indeed, if one looks more closely into the model structures reported by Horrocks *et al.*, one also gets a range of 4.5–5 by our definition of zinc coordination number. Hence, the earlier zinc model compounds reported also correlate with the overall zinc coordination pattern outlined above.

Discussion

The combined results of the structural studies of the CPA complexes described above may be used to clarify some of the general binding factors (of both inhibitors, substrates and analogues) for zinc proteinases. Although the benzyl succinate inhibitor [(I)], the keto-methylene pseudo-peptides [(II), (IV), (V)] and the phenolate inhibitors [(VIII), (IX)] present different molecular structures with significantly different binding moieties, their binding in the active site of the enzyme is rather similar. Especially striking are the similarities in their binding to the zinc and the two catalytic residues of the active site (Glu270 and Arg127) as demonstrated in a comparison of the active site of CPA bound to these three effectors. Fig. 13 presents a superposition of three such representative structures: the CPA complex with benzyl succinate [(I)], with keto-methylene analogue (II), and with phenolate inhibitor (VIII). Both (I) and (II) bind to the apical (or 'water accessible') side of the zinc as bidentate ligands, replacing the zinc-bound water, and both of them form good hydrogen bonds with Arg127 and Glu270. The A-carboxylate group of (I) and the *gem*-diolate group of (II) occupy an almost identical position of the active site and their O atoms form very similar coordination geometries relative to the zinc ion and its protein ligands. The tight binding of the two inhibitors is not surprising if one assumes that both structures resemble the actual catalytic tetrahedral intermediate in much the same way as the

zinc proteinases inhibitors phosphonate analogues mimic the tetrahedral intermediate (Hanson, Kaplan & Bartlett, 1989; Kaplan & Bartlett, 1991; Kim & Lipscomb, 1991).

Although the phenolate inhibitor (VIII) is a monodentate ligand, it binds the zinc in a fashion similar to that shown by (I) and (II). Binding of (VIII) displaces the zinc-bound water but the final position of the phenolate O atom correlates better with the other apical zinc-binding site [the position of O2 in both the carboxylate of (I) and the *gem*-diolate of (II)] rather than the expected position of the displaced water [which is also the position of O1 in both the carboxylate of (I) and the *gem*-diolate of (II)]. Occupying this position, the phenolate O atom comes into close proximity to Arg127, forming an additional interaction that potentially stabilizes a negative charge on the O atom and contributes further binding stabilization to the enzyme–inhibitor complex.

These results clarify some of the roles that various active-site residues, and especially the zinc ion, play in the binding of substrates and inhibitors, as well as in the stabilization of possible charged intermediates and/or transition states which develop along the catalytic reaction pathway of zinc proteinases. The zinc ion appears to influence, at least in part, the direct binding of substrates to the enzyme. The presence of other positively charged residues in the active site (*e.g.* Arg71, Arg127 and Arg145, and even His69 and His196) seems to be insufficient to bind substrates or inhibitors as effectively if the zinc is removed. CPA active-site residues Arg127 and Glu270, and to some extent Arg145, appear to play a role in stabilizing the transition states that evolve during the course of the reaction, as deduced by the interactions these residues make with the bound inhibitors. Since residues of similar characteristics and geometry are present in other zinc proteinases these roles may well be general for the mode of action of this enzyme family.

The comparison of the zinc environment in the various complexes of CPA with zinc model compounds seems to clarify the role of the zinc preferred coordination number and coordination geometry in the binding of various effectors to the enzyme. Fig. 14 shows a superposition of all of the zinc model compounds [(X), (XI), (XII) and (XIII)] and all of the CPA–inhibitor complexes [CPA/(I),

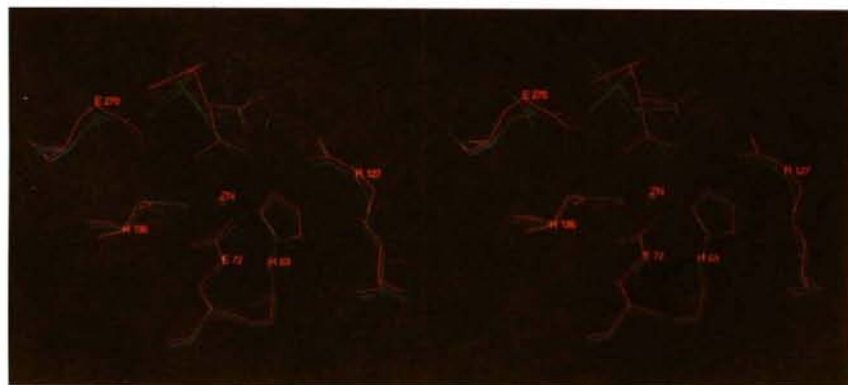


Fig. 13. A comparison of the CPA active site complexed with (I) (red), the active site complexed with (II) (blue) and the active site complexed with (VIII) (green).

CPA/(II), CPA/(V), CPA/(VIII) and CPA/(IX)] presented in this paper. Such superposition clearly demonstrates that the overall coordination of the zinc is generally similar in all of these structures. It seems that there are six preferred coordination sites, arranged in a non-classical distorted geometry around the zinc ion. Two of these sites are generally fixed in the coordination sphere of the zinc ion and occupied by nitrogen-donating heterocycles (His69 and His196 of the enzyme) each forming a rather short and direct single Zn—N bond. The other four sites are grouped into two pairs of sites. Each of these pairs can be fully coordinated (two full Zn—O interactions), or partially coordinated with either only one full Zn—O interaction or a combination of one full and one partial Zn—O interactions. In total, these two pairs of oxygen-binding sites could be fully occupied (total of four Zn—O full interactions) or only half occupied (total of two Zn—O full interactions), but the observed structures indicate that the preferred coordination of these two pairs of sites averages around three full interactions. Moreover, it seems that the coordination mode observed in one of the two pairs of sites is correlated with the coordination mode in the other pair of sites.

In the active site of CPA one such pair of oxygen coordination sites is occupied by Glu72 while the other pair of sites faces the opening of the active site into the solvent and is reserved for non-protein ligands. The structural data presented above demonstrates that the coordination of Glu72 in the first pair of sites is correlated with both the coordination number and the charge density of the non-protein ligand. From these data it seems that the effective coordination number of Glu72 decreases with the increase in the effective coordination number and/or the negative charge density of the non-protein ligand(s) bound to the zinc ion. A clear example for this pattern is demonstrated in the comparison of the CPA complex with inhibitor (I) with the CPA complexes with inhibitors (II) and (V). In the CPA/(I) complex the inhibitor carboxylate forms two full interactions with the zinc causing Glu72 to shift into

its monodentate conformation. In the CPA/(V) complex the analogue *gem*-diolate forms one full and one partial interaction forcing Glu72 to rotate only partially from its full double coordination to an intermediate state with one full and one partial interaction. Similarly, in the CPA/(II) complex the analogue *gem*-diolate forms only one full interaction with the zinc ion forcing Glu72 to rotate only slightly from its original doubly coordinated conformation. The complexes of CPA with the phenolate inhibitors [(VIII) and (IX)] seem to present an exception to this pattern since the non-protein ligand forms only one full interaction with the zinc ion, yet Glu72 rotates significantly out of its doubly coordinated position (such that one of the O atoms forms only a rather weak interaction with the zinc ion with a distance of 2.8 Å). Nevertheless, as indicated above, this decrease in the effective coordination of Glu72 can be explained in this case on the basis of the different nature of the charge of the phenolate O atom compared to the carboxylate or *gem*-diol groups of the other effectors discussed above.

Our results suggest, therefore, that the coordination of Glu72 to the zinc ion of CPA is quite flexible and closely correlated to the nature of interaction between the non-protein ligand and the zinc ion. Since non-protein ligands may also be substrates, transition states or products, the flexibility in both the conformation of Glu72 and its coordination to the zinc ion can be used by the enzyme to optimize binding to such species in catalysis. Such fine tuning in the zinc coordination and its effective charge may, in principle, provide the modulation in the zinc ion characteristics along the reaction coordinate which allows for the attraction and binding of the substrate, the stabilization of the transition state and the release of the products.

Recent extended X-ray absorption fine-structure spectroscopy results support the proposed flexibility in the coordination of Glu72 to the catalytic zinc ion in CPA (Zhang, Chance, Auld, Larsen & Vallee, 1992). The first coordination sphere of the zinc ion in solution is found to consist of two types of zinc–ligand distances. Four liganding atoms (either N or O) are shown to be located

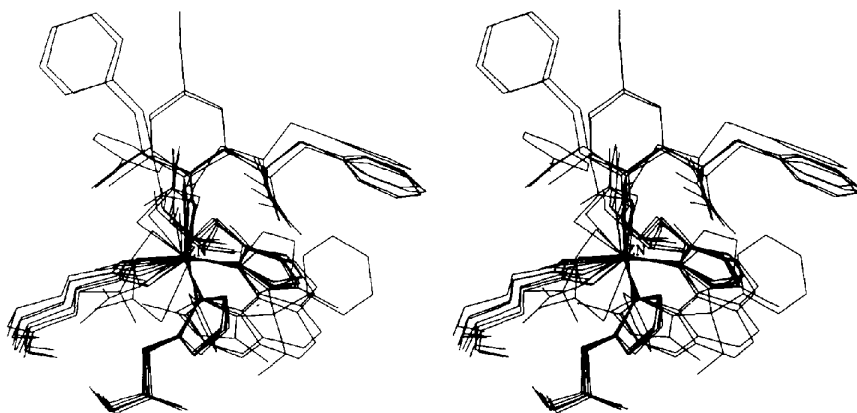


Fig. 14. Superposition of the zinc environments in native CPA, in CPA complexed with (I), (II), (V), (VIII), (IX) and in the zinc model compounds (X), (XI), (XII), (XIII) (superposition is based on the zinc ion and its coordinated N atoms).

at an average distance of 2.03 Å from the zinc ion, while a fifth liganding atom (either N or O) is shown to be located 2.57 Å from the zinc ion. The four atoms at an average distance of 2.03 Å are assigned to two N^δ atoms of His69 and His196 (N1 and N2), one O^ε atom of Glu72 (O1) and the O atom of the zinc-bound water (O3). The fifth ligated atom which is observed at 2.57 Å from the zinc ion in solution and assigned to the second O^ε atom of Glu72 (O2). These results, when compared to the crystallographic results presented above, suggest that even in slightly different conditions of native CPA (*e.g.* pH and ionic strength) the carboxylate group of Glu72 is flexible enough to rotate from a symmetrical coordination to a non-symmetrical coordination with the zinc ion.

Summary and conclusions

The experimental data presented and reviewed above concerning the mode of binding of the zinc ion in CPA are by no means complete or sufficient. Nevertheless, this information should be applicable for three different stages of rational inhibitor design: the improvement of CPA inhibitors, the improvement of inhibitors for other structurally known zinc proteinases of the CPA subgroup (ZP-H2E), and the design of first-generation inhibitors for enzymes of unknown structure from this subgroup.

The results obtained from study of the model compounds for ZP-H2E enzymes suggest that zinc coordination in the active site of these enzymes is not significantly strained by the protein environment and hence the significance of a zinc 'entatic state' (Vallee *et al.*, 1983) and its role in substrate binding and catalysis should be investigated further. These conclusions are based on careful structural analyses of our zinc-ligand models. Such model studies may be of great importance in the initial cycle of inhibitor design for these enzymes, since the zinc-binding mode and coordination geometry of various ligands may be initially examined in a series of model compounds prior to synthesis and analysis of the actual inhibitors.

The combined structural results obtained from the model compounds and the CPA complexes indicate that the effective coordination number of the zinc ion in ZP-H2E enzymes is 5 and that the coordination of the protein glutamic acid ligand is flexible enough to enable an efficient binding of both monodentate and bidentate ligands. Thus, in terms of the absolute binding values to the enzyme it seems that there is no significant advantage to bidentate zinc ligands over the monodentate zinc ligands. Nevertheless, the bidentate ligands offer a more specific binding to the zinc in the active-site environments of the ZP-H2E subgroup. Hence, these ligands are expected to be more selective towards this class of enzymes within the four families of proteinases in general, and within the family of zinc proteinases in particular.

The structural results obtained from the studies of the benzyl succinate complexes of CPA confirm that a second inhibitor carboxylate could serve as a strong bidentate ligand to the zinc ion. The results show that the zinc-binding carboxylate also interacts with specific amino-acid side chains in the active site and thus further stabilize this zinc-inhibitor complex formed. However, these studies also point out the limitations in such a zinc-binding moiety in terms of further potential inhibitor design with structural extensions into the P1 and P2 binding sites of the enzyme (Abramowitz *et al.*, 1967). In this respect, the keto-methylene inhibitors provide a much better starting model for the rational improvement of inhibitors. Their uncleaved keto-methylene group is turned by the enzyme into a *gem*-diolate which then acts as a relatively high-affinity zinc-directed bidentate group. In addition to the zinc, the resulting *gem*-diolate group can take full advantage of the binding interactions with the other catalytic residues in the active site (Glu270 and Arg127 in the case of CPA). The enzyme-binding capabilities of the *gem*-diolate moiety can then be used as a starting point for the extension and optimization of the amino-acid residues in the P1-P4 sites (in exopeptidases) or the addition of amino acids in the P1'-P4' sites (in endopeptidases).

The results obtained with the phenol-based derivatives demonstrate that potent inhibitors for CPA and other zinc proteinases do not necessarily have to resemble intermediates or transition states in the reaction pathway. This particular class of inhibitors provides an example for other features of zinc binding which may be utilized in inhibitor design. The delocalization of charge in the phenol ring of these inhibitors, a feature not present in other inhibitors, presumably makes a significant contribution to the relatively high affinity these molecules exhibit for zinc proteinases (Mock & Aksamawati, 1994). This family of inhibitors provides a novel starting point for the design of more potent and selective inhibitors, which would certainly be advantageous. In addition to substituents on the phenol ring which might resemble extensions to a polypeptide chain, and so impart selectivity, other substituents could fine tune the affinity the inhibitor has for the zinc through the factors mentioned above. In this sense, this family of compounds has a distinct advantage over others, where the only significant modifications can be in the extended binding site, but not in the affinity for the metal ion itself.

We would like to express our gratitude to W. L. Mock who kindly supplied us with the phenolate inhibitors used in these studies. We thank A. J. Bauer for critically reading this manuscript and for his valuable corrections. We thank P. Tucker for his important technical assistance with the crystallographic data measurement of several of the CPA derivatives. We thank S. L. Lippard who kindly supplied us with the ligand BIPhMe. We acknowledge the Unit of Inter-departmental Services of the Institute of

Life Sciences for providing us with some of the equipment needed for biochemical analysis. We thank the Israeli Academy of Sciences (grant No. 253/88), the Friends of the Hebrew University in England and Ms Myrtle Franklin, and the Bat Sheva de Rothchild Foundation for financial support. One of us (HF) thanks the Wolf Foundation and the Levi Eshkol Foundation for graduate studies scholarship, and one of us (HMG) thanks the Pulver Foundation for general financial support.

References

- ABRAMOWITZ, N., SCHECHTER, I. & BERGER, A. (1967). *Biochem. Biophys. Res. Commun.* **29**, 862–867.
- BAUMANN, U., WU, S., FLAHERTY, K. M. & MCKAY, D. B. (1993). *EMBO J.* **12**, 3357–3364.
- BERTINI, I., LUCHINAT, C. & VIEZZOLI, M. S. (1986). *Metal Substitution as a Tool for the Investigation of Zinc Proteins*, in *Zinc Enzymes*, PBB Vol. 1, pp. 27–47. Boston: Birkhauser.
- BICKNELL, R., SCHAFFER, A., BERTINI, I., LUCHINAT, C., VALLEE, B. L. & AULD, D. S. (1988). *Biochemistry*, **27**, 1050–1057.
- BLUNDELL, T. L. (1994). *Nature Struct. Biol.* **1**, 73–75.
- BODE, W., GOMIS-RUETH, F. X., HUBER, R., ZWILLING, R. & STOCKER, W. (1992). *Nature (London)*, **358**, 164–167.
- BODE, W., REINEMER, P., HUBER, R., KLEINE, T., SCHNEIERER, S. & TSCHESCHE, H. (1994). *EMBO J.* **13**, 1263–1269.
- BOLOGNESI, M. C. & MATTHEWS, B. W. (1979). *J. Biol. Chem.* **254**, 634–639.
- BORKAKOTI, N., WINKLER, F. K., WILLIAMS, D. H., D'ARCY, A., BROADHURST, M. J., BROWN, P. A., JOHNSON, W. H. & MURRAY, E. J. (1994). *Nature Struct. Biol.* **1**, 106–110.
- BURLEY, S. K., DAVID, P. R., SWEET, R. M., TAYLOR, A. & LIPSCOMB, W. N. (1992). *J. Mol. Biol.* **224**, 113–140.
- BYERS, L. D. & WOLFENDEN, R. (1972). *J. Biol. Chem.* **247**, 606–608.
- BYERS, L. D. & WOLFENDEN, R. (1973). *Biochemistry*, **12**, 2070–2078.
- CHEVRIER, B., SCHALK, C., D'ORCHYMONT, H., RONDEAU, J.-M., MORAS, D. & TARNUS, C. (1994). *Structure*, **2**, 283–291.
- CHRISTIANSON, D. W. (1991). *Adv. Protein Chem.* **42**, 281–353.
- CHRISTIANSON, D. W., DAVID, P. R. & LIPSCOMB, W. N. (1987). *Proc. Natl Acad. Sci. USA*, **84**, 1512–1515.
- CHRISTIANSON, D. W. & LIPSCOMB, W. N. (1985a). *Proc. Natl Acad. Sci. USA*, **82**, 6840–6844.
- CHRISTIANSON, D. W. & LIPSCOMB, W. N. (1985b). *J. Am. Chem. Soc.* **107**, 8281–8283.
- CHRISTIANSON, D. W. & LIPSCOMB, W. N. (1986a). *J. Am. Chem. Soc.* **108**, 545–546.
- CHRISTIANSON, D. W. & LIPSCOMB, W. N. (1986b). *J. Am. Chem. Soc.* **108**, 4998–5003.
- CHRISTIANSON, D. W. & LIPSCOMB, W. N. (1987). *J. Am. Chem. Soc.* **109**, 5536–5538.
- CHRISTIANSON, D. W. & LIPSCOMB, W. N. (1989). *Acc. Chem. Res.* **22**, 62–69.
- CHRISTIANSON, D. W., MANGANI, S., SHOHAM, G. & LIPSCOMB, W. N. (1989). *J. Biol. Chem.* **264**, 12849–12853.
- COLEMAN, J. E. & VALLEE, B. L. (1962). *J. Biol. Chem.* **237**, 3430–3436.
- CUSHMAN, D. W., CEUNG, H. S., SABO, E. F. & ONDETTI, M. A. (1977). *Biochemistry*, **16**, 5484–5491.
- DIDEBERG, O., CHARLIER, P., DIVE, G., JORIS, B., FRERE, J. M. & GHUYSEN, J. M. (1982). *Nature (London)*, **299**, 469–470.
- EWENSON, A., COHEN-SLISSA, R., LEVIAN-TEITELBAUM, D., SELINGER, Z., CHOREV, M. & GILON, C. (1988). *Int. J. Peptide Protein Res.* **31**, 269–280.
- EWENSON, A., LAUFER, R., CHOREV, M., SELINGER, Z. & GILON, C. (1988). *J. Med. Chem.* **31**, 416–421.
- FAMING, Z., KOBE, B., RUTTER, W. J. & GOLDSMITH, E. J. (1991). *J. Biol. Chem.* **266**, 24606–24612.
- FEINBERG, H., GREENBLATT, H. M. & SHOHAM, G. (1995). In preparation.
- FEINBERG, H., GREENBLATT, H. M. & SHOHAM, G. (1993). *J. Chem. Inf. Comput. Sci.* **33**, 501–516.
- GILMORE, G. J. (1984). *J. Appl. Cryst.* **17**, 42–46.
- GILSON, M. K. & HONIG, B. H. (1987). *Nature (London)*, **330**, 84–86.
- GILSON, M. K., SHARP, K. A. & HONIG, B. H. (1988). *J. Comp. Chem.* **9**, 327–335.
- GLUSKER, J. P. (1991). *Adv. Protein Chem.* **42**, 1–76.
- GOMIS-RUETH, F. X., KRESS, L. F. & BODE, W. (1993). *EMBO J.* **12**, 4151–4157.
- GOMIS-RUETH, F. X., STOCKER, W., HUBER, R., ZWILLING, R. & BODE, W. (1993). *J. Mol. Biol.* **229**, 945–968.
- GOOLEY, P. R., O'CONNELL, J. F., MARCY, A. I., CUCA, G. C., SALOWE, S. P., BUSH, B. L., HERMES, J. D., ESSER, C. K., HAGMANN, W. K., SPRINGER, J. P. & JOHNSON, B. A. (1993). *Biochemistry*, **32**, 13098–13108.
- GOOLEY, P. R., O'CONNELL, J. F., MARCY, A. I., CUCA, G. C., SALOWE, S. P., BUSH, B. L., HERMES, J. D., ESSER, C. K., HAGMANN, W. K., SPRINGER, J. P. & JOHNSON, B. A. (1994). *Nature Struct. Biol.* **1**, 111–118.
- GREENBLATT, H. M., FEINBERG, H., TUCKER, P. & SHOHAM, G. (1995). In preparation.
- GROVES, J. T. & BARON, L. A. (1989). *J. Am. Chem. Soc.* **111**, 5442–5448.
- GROVES, J. T. & CHAMBERS, R. R. JR (1984). *J. Am. Chem. Soc.* **106**, 630–638.
- GROVES, J. T. & OLSON, J. R. (1985). *Inorg. Chem.* **24**, 2717–2720.
- HANSON, J. E., KAPLAN, A. P. & BARTLETT, P. A. (1989). *Biochemistry*, **28**, 6294–6305.
- HARADA, S., KITADOKORO, K., KINOSHITA, T., KAI, Y. & KASSAI, N. (1991). *J. Biochem.* **110**, 46–49.
- HENDRICKSON, W. A. & KONNERT, J. (1981). In *Biomolecular Structure. Function. Conformation and Evolution*, edited by R. SRINIVASAN, Vol. 1, pp. 43–47. Oxford: Pergamon Press.
- HOLMES, M. A. & MATTHEWS, B. W. (1982). *J. Mol. Biol.* **160**, 623–639.
- HORROCKS, W. D., ISHLEY, J. N., HOLMQUIST, B. & THOMPSON, S. (1980). *J. Inorg. Biochem.* **12**, 131–141.
- HORROCKS, W. D., ISHLEY, J. N. & WHITTLE, R. R. (1982a). *Inorg. Chem.* **21**, 3270–3274.
- HORROCKS, W. D., ISHLEY, J. N. & WHITTLE, R. R. (1982b). *Inorg. Chem.* **21**, 3265–3269.
- JERNIGAN, R., RAGHUNATHAN, G. & BAHAR, I. (1994). *Curr. Op. Struct. Biol.* **4**, 256–263.
- KAPLAN, A. P. & BARTLETT, P. A. (1991). *Biochemistry*, **30**, 8165–8170.
- KARLIN, K. (1993). *Science*, **261**, 701–708.
- KIM, H. & LIPSCOMB, W. N. (1991). *Biochemistry*, **30**, 8171–8180.
- KIM, H. & LIPSCOMB, W. N. (1993). *Proc. Natl Acad. Sci. USA*, **90**, 5006–5010.
- KIMURA, E. (1994). *Progr. Inorg. Chem.* **41**, 442–491.
- LE HUROU, I., GUILLLOTEAU, P., TOULLEC, R., PUISSERVER, A. & WICKER, C. (1991). *Biochem. Biophys. Res. Commun.* **175**, 110–116.
- LIPSCOMB, W. N. (1980). *Proc. Natl Acad. Sci. USA*, **77**, 3875–3878.
- LIPSCOMB, W. N., HARTSLUCK, J. A., REEKE, G. J., QUIOCHO, F. A., BETHGE, P. H., LUDWIG, M. L., STEITZ, T. A., MUIRHEAD, H. & COPPOLA, J. C. (1968). *Brookhaven Symp. Biol.* **21**, 24–90.
- LOVEJOY, B., CLEASBY, A., HASSELL, A. M., LONGLEY, K., LUTHER, M. A., WEIGL, D., MCGEEHAN, G., MCELROY, A. B., DREWRY, D., LAMBERT, M. H. & JORDAN, S. R. (1994). *Science*, **263**, 375–377.
- MALFROY, B., SWERTS, J. P., GUYON, A., ROQUES, B. P. & SCHWARTZ, J. C. (1978). *Nature (London)*, **276**, 523–526.
- MANGANI, S., CARLONI, P. & ORIOLI, P. (1992a). *J. Mol. Biol.* **223**, 573–578.
- MANGANI, S., CARLONI, P. & ORIOLI, P. (1992b). *Eur. J. Biochem.* **203**, 173–177.
- MANGANI, S. & ORIOLI, P. (1992). *Inorg. Chem.* **31**, 365–368.
- MARET, W. (1986). *Methodology of Metal Exchange in Metalloproteins*. In *Zinc Enzymes*, PBB Vol. 1, pp. 17–26. Boston: Birkhauser.
- MARTIN, M. T., HOLMQUIST, B. & RIORDAN, J. F. (1989). *J. Inorg. Biochem.* **36**, 27–37.
- MOCK, W. L. & AKSAMAWATI, M. (1994). *Biochem. J.* **302**, 57–68.

- MOCK, W. L., FREEMAN, D. J. & AKSAMAWATI, M. (1993). *Biochem. J.* **298**, 185–193.
- MOCK, W. L. & TSAY, J.-T. (1986). *Biochemistry*, **25**, 2920–2927.
- MOCK, W. L. & TSAY, J.-T. (1988). *J. Biol. Chem.* **263**, 8635–8641.
- Molecular Structure Corporation (1985). *TEXSAN. TEXRAY Structure Analysis Package*, MSC, 3200 Research Forest Drive, The Woodlands, TX 77381, USA.
- MOTHERWELL, S. & CLEGG, W. (1978). *PLUTO. Program for the Plotting of Molecular and Crystal Structures*. Univ. of Cambridge, England.
- NEURATH, H., BRADSHAW, R. A., PÉTRA, P. H. & WALSH, K. A. (1970). *Philos. Trans. R. Soc. London Ser. B*, **257**, 159–176.
- ONDETTI, M. A. & CUSHMANN, D. W. (1982). *Ann. Rev. Biochem.* **51**, 283–308.
- PATCHETT, A. A. HARRIS, E., TRISTRAM, E. W., WYVRATT, M. J., WU, M. T., TAUB, D., PETERSON, E. R., IKELER, T. J., BROEKE, J., PAYNE, L. G., ONDEYKA, D. L., THOSETT, E. D., GREENLEE, W. J., LOHR, N. S., HOFFSOMMER, R. D., JOSHUA, H., RUYLE, W. V., ROTHROCK, J. W., ASTER, S. D., MAYCOCK, A. L., ROBINSON, F. M., HIRSCHMANN, R., SWEET, C. S., ULM, E. H., GROSS, D. M. VASSIL, T. C. & STONE, C. A. (1980). *Nature (London)*, **288**, 280–283.
- PAUPTIT, R. A., KARLSSON, R., PICOT, D., JENKINS, J. A., NIKLAUS-REIMER, A. S. & JANSONIUS, J. N. (1988). *J. Mol. Biol.* **199**, 525–537.
- PÉTRA, P. H., HERMODSON, M. A., WALSH, K. A. & NEURATH, H. (1971). *Biochemistry*, **10**, 4023–4025.
- PHILLIPS, M. A., FLETTERICK, R. & RUTTER, W. J. (1990). *J. Biol. Chem.* **265**, 20692–20698.
- QUIOCHO, F. A., McMURRAY, C. H. & LIPSCOMB, W. N. (1972). *Proc. Natl Acad. Sci. USA*, **69**, 2850–2854.
- QUIOCHO, F. A. & RICHARDS, F. M. (1966). *Biochemistry*, **5**, 4062–4076.
- REES, D. C., LEWIS, M. & LIPSCOMB, W. N. (1983). *J. Mol. Biol.* **168**, 367–387.
- REES, D. C. & LIPSCOMB, W. N. (1982). *J. Mol. Biol.* **160**, 475–498.
- REES, D. C. & LIPSCOMB, W. N. (1983). *Proc. Natl Acad. Sci. USA*, **80**, 7151–7154.
- SARKAR, B. (1977). *Metal-Ligand Interactions in Organic Chemistry and Biochemistry*, edited by B. PULLMAN & N. D. GOLDBLUM, Part 1, pp. 193–228. Dordrecht, The Netherlands: Reidel.
- SATO, M., YAMAMOTO, M., IMADA, K., KATSUBE, Y., TANAKA, N. & HIGASHI, T. A. (1992). *J. Appl. Cryst.* **25**, 348–357.
- SCHMID, M. F. & HERRIOTT, J. R. (1976). *J. Mol. Biol.* **103**, 175–190.
- SCHWARTZ, J. C., GROS, C., LECOMTE, J. M. & BRALET, J. (1990). *Life Sci.* **47**, 1279–1297.
- SHELDRIK, G. M. (1985). *SHELXS in Crystallographic Computing 3*, edited by G. M. SHELDRIK, C. KRUGER & R. GODDARD, pp. 175–189. Oxford Univ. Press.
- SHIBATA, A. (1990). *Rigaku J.* **7**, 28–32.
- SHOHAM, G., CHRISTIANSON, D. W. & OREN, D. A. (1988). *Proc. Natl Acad. Sci. USA*, **85**, 684–688.
- SHOHAM, G., OREN, D. A., EWENSON, A. & GILON, C. (1988). *Inhibition of Carboxypeptidase A with Keto-methylene Pseudopeptides. Proceedings of the 20th European Peptide Symposium*, pp. 411–413. Tübingen: Walter de Gruyter.
- SHOHAM, G., REES, D. C. & LIPSCOMB, W. N. (1984). *Proc. Natl Acad. Sci. USA*, **81**, 7767–7771.
- SOFFER, R. L. (1976). *Ann. Rev. Biochem.* **45**, 73–94.
- SPURLINO, J. C., SMALLWOOD, A. M., CARLTON, D. D., BANKS, T. M., VAVRA, K. J., JOHNSON, J. S., COOK, E. R., FALVO, J., WAHL, R. C., PULVINO, T. A., WENDOLOSKI, J. J. & SMITH, D. L. (1994). *Proteins*, **19**, 98–109.
- STAMS, T., SPURLINO, J. C., SMITH, D. L., WAHL, R. C., HO, T. F., QOROFLEH, M. W., BANKS, T. M. & RUBIN, B. (1994). *Nature Struct. Biol.* **1**, 119–123.
- STARK, W., PAUPTIT, R. A., WILSON, K. S. & JANSONIUS, J. N. (1992). *Eur. J. Biochem.* **207**, 781–791.
- TEPLYAKOV, A., POLYAKOV, K., OBMOLOVA, G., STROKOPYTOV, B., KURANOVA, I., OSTERMAN, A., GRISHIN, N., SMULEVITCH, S., ZAGNITKO, O., GALPERINA, O., MATZ, M. & STEPANOV, V. (1992). *Eur. J. Biochem.* **208**, 281–288.
- THAYER, M. M., FLAHERTY, K. M. & MACKAY, D. B. (1991). *J. Biol. Chem.* **266**, 2864–2871.
- VALLEE, B. L. (1986). *A Synopsis of Zinc Biology and Pathology*. In *Zinc Enzymes*, PBB Vol. 1, pp. 1–15. Boston: Birkhauser.
- VALLEE, B. L. & AULD, D. S. (1993a). *Acc. Chem. Res.* **26**, 543–551.
- VALLEE, B. L. & AULD, D. S. (1993b). *Biochemistry*, **32**, 6494–6500.
- VALLEE, B. L. & GALDES, A. (1984). *Adv. Enzymol.* **56**, 283–430.
- VALLEE, B. L., GALDES, A., AULD, D. S. & RIORDAN, J. F. (1983). *Carboxypeptidase A*, in *Metal Ions in Biology*, edited by T. G. SPIRO, Vol. 5, pp. 25–75. New York: John Wiley.
- WALKER, N. & STUART, D. (1983). *Acta Cryst.* **A39**, 158–166.
- WOLLEY, P. (1975). *Nature (London)*, **258**, 677–682.
- ZHANG, K., CHANCE, B., AULD, D. A., LARSEN, K. S. & VALLEE, B. L. (1992). *Biochemistry*, **31**, 1159–1168.